

# ScholarWorks@GSU

## Microbial Biofilms: An Evaluation of Ecological Interactions and the Use of Natural Products as Potential Therapeutic Agents

Authors	Santiago, Ariel J.
Citation	Santiago, Ariel J.. 2016. "Microbial Biofilms: An Evaluation of Ecological Interactions and the Use of Natural Products as Potential Therapeutic Agents." Georgia State University. <a href="https://doi.org/10.57709/9431702">https://doi.org/10.57709/9431702</a>
DOI	<a href="https://doi.org/10.57709/9431702">https://doi.org/10.57709/9431702</a>
Download date	2026-03-06 20:55:39
Link to Item	<a href="https://hdl.handle.net/20.500.14694/1982">https://hdl.handle.net/20.500.14694/1982</a>

MICROBIAL BIOFILMS: AN EVALUATION OF ECOLOGICAL INTERACTIONS AND  
THE USE OF NATURAL PRODUCTS AS POTENTIAL THERAPEUTIC AGENTS

by

ARIEL J. SANTIAGO

Under the Direction of Eric S. Gilbert, PhD

ABSTRACT

Biofilms are communities of microorganisms associated with surfaces encased in a protective extracellular matrix. These communities often pose clinical and industrial challenges due to their ability to tolerate biocidal treatments and removal strategies. Understanding the ecological interactions that take place during biofilm establishment is a key element for designing future treatment strategies. In this work, I utilized unique methods for studying factors contributing to cooperative antibiotic detoxification in a polymicrobial biofilm model. Subsequently, I tested a novel compound mixture that exhibited promising antibiofilm properties. Escapin is an L-amino acid oxidase that acts on lysine to produce hydrogen peroxide (H<sub>2</sub>O<sub>2</sub>),

ammonia, and equilibrium mixtures of several organic acids collectively called Escapin intermediate products (EIP). Previous work showed that the combination of synthetic EIP and H<sub>2</sub>O<sub>2</sub> functions synergistically as an antimicrobial toward diverse planktonic bacteria. To test the combination of EIP and H<sub>2</sub>O<sub>2</sub> on bacterial biofilms, *Pseudomonas aeruginosa* was selected as a model, due to its role as an important opportunistic pathogen. Specifically, I examined concentrations of EIP and H<sub>2</sub>O<sub>2</sub> that inhibited biofilm formation or fostered disruption of established biofilms. High-throughput assays of biofilm formation using microtiter plates and crystal violet staining showed a significant effect from pairing EIP and H<sub>2</sub>O<sub>2</sub>, resulting in inhibition of biofilm formation relative to untreated controls or to EIP or H<sub>2</sub>O<sub>2</sub> alone. Similarly, flow cell analysis and confocal laser scanning microscopy revealed that the EIP and H<sub>2</sub>O<sub>2</sub> combination reduced the biomass of established biofilms relative to controls. Area layer analysis of biofilms post-treatment indicated that disruption of biomass occurs down to the substratum. Only nanomolar to micromolar concentrations of EIP and H<sub>2</sub>O<sub>2</sub> were required to impact biofilm formation or disruption, which are significantly lower concentrations than those causing bactericidal effects on planktonic bacteria. Micromolar concentrations of EIP and H<sub>2</sub>O<sub>2</sub> combined enhanced *P. aeruginosa* swimming motility compared to either EIP or H<sub>2</sub>O<sub>2</sub> alone. Collectively, these results suggest that the combination of EIP and H<sub>2</sub>O<sub>2</sub> may affect biofilms by interfering with bacterial attachment and destabilizing the biofilm matrix.

INDEX WORDS: Biofilms, *Escherichia coli*, *Pseudomonas aeruginosa*, escapin, hydrogen peroxide, natural products, biofilm inhibition, biofilm dispersal

MICROBIAL BIOFILMS: AN EVALUATION OF ECOLOGICAL INTERACTIONS AND  
THE USE OF NATURAL PRODUCTS AS POTENTIAL THERAPEUTIC AGENTS

by

ARIEL J. SANTIAGO

A Dissertation Submitted in Partial Fulfillment of the Requirements for the Degree of

Doctor of Philosophy

in the College of Arts and Sciences

Georgia State University

2016

Copyright by  
Ariel José Santiago  
2016

MICROBIAL BIOFILMS: AN EVALUATION OF ECOLOGICAL INTERACTIONS AND  
THE USE OF NATURAL PRODUCTS AS POTENTIAL THERAPEUTIC AGENTS

by

ARIEL J. SANTIAGO

Committee Chair: Eric S. Gilbert

Committee: George E. Pierce

Sidney A. Crow Jr.

Charles D. Derby

Electronic Version Approved:

Office of Graduate Studies

College of Arts and Sciences

Georgia State University

December 2016

## DEDICATION

This work is dedicated to my grandparents: Valeriano Santiago, Velia Sánchez, Francisco Sosa and Teresa Rojas, who taught me, through their example, the importance of humility, hard work and a passion for education. I would also like to dedicate this work to my family: Elmer Santiago and Widalys Sosa (parents), Pablo Santiago, Ramón Bargalló, Elmer Santiago Jr., Eric Santiago, Widalys Santiago and Caroline Santiago (siblings) for your support during my academic endeavors. Additionally, I would like to thank my partner Judith Kërr and her family for their support throughout these years. Lastly, I want to dedicate this work to the memory of Dr. Pedro Albizu Campos and the belief that one day the people of Puerto Rico will wake up to a free and sovereign nation.

## ACKNOWLEDGEMENTS

I would like to begin by thanking my advisor Dr. Eric S. Gilbert for his guidance throughout the completion of my graduate work. I would like to thank my committee members Drs. George Pierce, Sidney Crow Jr. and Charles Derby for their insights, advice and guidance. I would like to thank Dr. P.C. Tai for his valuable mentorship during the latter part of my graduate work. I would like to thank Dr. Barbara Baumstark and the Bio-Bus Program for making my venture into graduate school possible and providing an opportunity to exercise my passion for science education. I would like to thank Dr. Robert Simmons for training and use of the confocal microscope. I would like to thank Drs. Robert Maxwell and Jeanetta Floyd for helping me to enhance my teaching experience throughout my graduate work. I would like to acknowledge my research colleagues: Dr. Bryan A. Stubblefield, Dr. Chandan Morris, Dr. Fengkun Du, Dr. Bianca Islam, Dr. Kristen Howery, Dr. Emory Gray, Dave Martin, Casey Seldon, Marwa Ahmed, Hsiuchin Yang, Shu-Lin Wang, Vivian Ngo-Vu, Chia-Ching Lin, Chun-Yi Lai, and Dr. Mariya Campbell. Lastly, I would like to thank the Department of Biology as well as the Georgia Research Alliance for financial support throughout the years.

## TABLE OF CONTENTS

<b>ACKNOWLEDGEMENTS .....</b>	<b>v</b>
<b>LIST OF FIGURES .....</b>	<b>ix</b>
<b>1 INTRODUCTION .....</b>	<b>1</b>
<b>1.1 Biofilms: diverse and complex communities of microorganisms.....</b>	<b>1</b>
<b>1.2 Antibiotic resistance: an evolutionary arms race.....</b>	<b>1</b>
<b>1.3 Natural products and the emergence of anti-virulence strategies .....</b>	<b>2</b>
<b>1.4 Objectives and hypotheses.....</b>	<b>3</b>
<i>1.4.1 Factors affecting polymicrobial biofilm establishment .....</i>	<i>3</i>
<i>1.4.2 The use of natural products as potential therapeutic agents .....</i>	<i>3</i>
<b>2 Factors affecting early stage polymicrobial biofilm formation in the presence of multiple antibiotics.....</b>	<b>5</b>
<b>2.1 Introduction .....</b>	<b>5</b>
<b>2.2 Materials and Methods .....</b>	<b>6</b>
<i>2.2.1 Strains and culture conditions.....</i>	<i>6</i>
<i>2.2.2 Cultivation of biofilms .....</i>	<i>7</i>
<i>2.2.3 Microscopy and image analysis .....</i>	<i>8</i>
<i>2.2.4 Statistical analysis .....</i>	<i>8</i>
<b>2.3 Results .....</b>	<b>9</b>
<i>2.3.1 Community-dependent antibiotic tolerance and biofilm establishment .....</i>	<i>9</i>

2.3.2	<i>Effects of areal density and antibiotic exposure on biofilm formation under antibiotic challenge: phosphate-recirculated cells</i> .....	11
2.3.3	<i>Effects of areal density and antibiotic exposure on biofilm formation under antibiotic challenge: LB-recirculated cells</i> .....	13
2.4	<b>Discussion</b> .....	15
3	<b>Inhibition and dispersal of <i>Pseudomonas aeruginosa</i> biofilms by combination treated of Escapin intermediate products and hydrogen peroxide.</b> .....	18
3.1	<b>Introduction</b> .....	18
3.2	<b>Materials and Methods</b> .....	20
3.2.1	<i>Culture preparation</i> .....	20
3.2.2	<i>Chemicals</i> .....	21
3.2.3	<i>Assay of biofilm formation</i> .....	22
3.2.4	<i>Assay of biofilm dispersal</i> .....	22
3.2.5	<i>Motility assays</i> .....	23
3.2.6	<i>Statistical analysis</i> .....	24
3.3	<b>Results</b> .....	25
3.3.1	<i>EIP + H<sub>2</sub>O<sub>2</sub> in combination inhibit <i>P. aeruginosa</i> biofilm formation at micromolar concentrations</i> .....	25
3.3.2	<i>EIP and H<sub>2</sub>O<sub>2</sub> work synergistically to disperse <i>P. aeruginosa</i> biofilms</i> .....	27
3.3.3	<i>Treatment with EIP or EIP + H<sub>2</sub>O<sub>2</sub> disperses but does not increase membrane damage within <i>P. aeruginosa</i> biofilm</i> .....	28

3.3.4	<i>EIP and EIP + H<sub>2</sub>O<sub>2</sub> disrupt the biofilm structure from substratum to apex</i>	
		<i>31</i>
3.3.5	<i>EIP and EIP + H<sub>2</sub>O<sub>2</sub> enhances P. aeruginosa swimming motility</i> .....	<i>31</i>
3.4	Discussion.....	35
4	CONCLUSIONS.....	40
	REFERENCES.....	43

**LIST OF FIGURES**

Figure 2.1: Community-dependent biofilm establishment under antibiotic challenge.....	10
Figure 2.2: Effects of areal density and antibiotic exposure on phosphate-recirculated cells in 24 h biofilm formation.....	12
Figure 2.3: Effects of areal density and antibiotic exposure on LB-recirculated cells in 24 h biofilm formation.....	14
Figure 3.1: Summary of the chemistry of the reaction of Escapin with L-lysine, including the effects of pH on the relative composition of the molecular species in the equilibrium mixture .....	20
Figure 3.2: Effects of EIP and H <sub>2</sub> O <sub>2</sub> on <i>P. aeruginosa</i> biofilm formation. ....	26
Figure 3.3: Effects of EIP on <i>P. aeruginosa</i> and biofilm cell viability and biomass. ....	28
Figure 3.4: Effects of EIP and H <sub>2</sub> O <sub>2</sub> on <i>P. aeruginosa</i> biofilm disruption.....	30
Figure 3.5: Effects of EIP on motility at 2 and 4 h... ..	33
Figure 3.6: Effects of EIP + H <sub>2</sub> O <sub>2</sub> on motility at 2 and 4 h. . . . .	34

## 1 INTRODUCTION

### 1.1 Biofilms: diverse and complex communities of microorganisms

The complexity of the microbial world is often oversimplified or misunderstood. This often leads to the common misconception that microorganisms exist as pure cultures of planktonic cells. Microorganisms, however, are more likely to exist in surface-attached, complex multispecies communities encased in a protective extracellular matrix (2). The composition of this matrix varies from species to species; however, it is generally composed of lipids, polysaccharides, nucleic acids, and proteins. The interplay between these components provides a three-dimensional structure that holds cells together (3), maintains key enzymes in their immediate environment (4), while providing protection from environmental threats (5).

In addition to the complexity of the biofilm structure and composition, the diversity of environments in which biofilms exist are well documented (6). From growth in hydrothermal vents to implanted medical devices, biofilms are able to establish and thrive in many environments. In many cases, however, their presence leads to economic loss (7, 8) as well as increased morbidity and mortality (9).

### 1.2 Antibiotic resistance: an evolutionary arms race

The discovery and development of antibiotics has undoubtedly changed the way humanity has dealt with bacterial infections for nearly three-quarters of a century. Unfortunately, widespread and indiscreet use of these drugs over the last 50-60 years has led to the emergence of antibiotic resistance among previously susceptible pathogenic strains (10, 11). The emergence of multi-drug resistant strains has led to a push for the development of alternative methods of chemotherapeutic treatments with the goal of reducing the incidence of resistance (12, 13). While research for

alternatives is both promising and ongoing, at present, the reliance on conventional antibiotics in clinical settings is still high. Chronic exposure to various types of antibiotics has provided a spark in an evolutionary “arms race” in which bacteria have developed mechanisms for the spread of resistance genes as well as stabilization of resistant phenotypes (11).

### **1.3 Natural products and the emergence of anti-virulence strategies**

The increase in prevalence of bacterial strains that are resistant to current antibiotic treatments has led to the emergence of anti-virulence strategies that can overcome many of the evolutionary-driven resistance mechanisms that currently exist (14). These strategies include screening small molecule libraries for antimicrobial effects (15), matrix degrading enzymes (16), antimicrobial surface coatings (17, 18), among others. In general, anti-virulence strategies aim to disrupt mechanisms or pathways that contribute to infection and disease while minimizing the evolutionary triggers that lead to drug-resistance (19).

Many of these biologically active compounds are naturally derived from vastly diverse sources. For example, plant-derived compounds such as cinnamaldehyde (essential oil) have been shown to disrupt biofilm formation in *Escherichia coli* and methicillin-resistant *Staphylococcus aureus* (20, 21) and reduce virulence in *Vibrio* spp. by interfering with quorum-sensing mechanisms (22). L-Amino acid oxidases and their enzymatic by-products, found in snake venom (23), the epidermal mucus of marine fish (24), and defensive secretions of marine invertebrates (25), have well-documented antimicrobial effects against both Gram-positive and Gram-negative pathogens through various mechanisms. The identification of these biologically active compounds and their prospective applications as chemotherapeutic agents will provide a major boost to the armament of drugs currently available.

## **1.4 Objectives and hypotheses**

### **1.4.1 Factors affecting polymicrobial biofilm establishment**

The objective of this work is to further our collective understanding of the factors affecting the establishment of polymicrobial biofilms. In many cases, the polymicrobial nature of these communities complicates treatment strategies and prolongs periods of disease (26). To this end, we have incorporated methods for studying initial polymicrobial formation in order to test the following hypotheses. 1) Colonization of a surface is key during initial biofilm formation. Therefore it is hypothesized that polymicrobial biofilm formation by antibiotic resistant strains could be enhanced by increasing the areal density, or the number of attached cells per microscopic field. The areal density of a constructed biofilm can be influenced by adjusting the inoculum density of the strains used during initial biofilm formation and thus can be used to model its overall impact. 2) Nutrient availability during biofilm formation could promote rapid growth of bacteria and ultimately influence biomass accumulation during biofilm formation. It is hypothesized that this increase in biomass accumulation would result in improved antibiotic tolerance in biofilms grown under antibiotic challenge. 3) Antibiotic exposure during early biofilm formation has been known to trigger biofilm formation (27). Thus, it was hypothesized that antibiotic exposure during early biofilm formation would enhance the antibiotic tolerance of strains forming biofilms under antibiotic challenge.

### **1.4.2 The use of natural products as potential therapeutic agents**

The use of bioactive natural products with antimicrobial properties has opened new avenues of treatment strategies for combating antibiotic resistance. One of these natural products known as escapin, is an L-amino acid oxidase that reacts with L-lysine to produce an equilibrium mixture of organic acids, hydrogen peroxide, and ammonium (1). These components were found

to exhibit antimicrobial properties against planktonic cultures of relevant bacterial pathogens (28) and as a result, it was hypothesized that the same components would exhibit inhibitory or dispersive effects towards bacterial biofilms. The work associated in this investigation used the opportunistic human pathogen *Pseudomonas aeruginosa* as a model.

## 2 Factors affecting early stage polymicrobial biofilm formation in the presence of multiple antibiotics

### 2.1 Introduction

Microorganisms are often perceived as free-floating cells that exist as single entities in their environment; however, they are more commonly found in structured, multispecies communities known as biofilms (29). Biofilms are typically characterized by their attachment to surfaces (biotic and abiotic) as well as their production of an extracellular polymeric matrix in which the microbial community is encapsulated. This protective matrix allows microorganisms to withstand adverse environmental conditions including biocidal treatments (30). Biofilms are ubiquitous in nature, and their presence extends to medical, environmental, and industrial settings.

The negative impact of biofilms is of particular importance in clinical settings. Biofilm communities, as well as their inherent resistance to antimicrobial agents, are at the root of many persistent and chronic bacterial infections (29). For example, biofilms of the human pathogen *Pseudomonas aeruginosa* are frequently responsible for chronic infections in cystic fibrosis patients (31). Another biofilm-based issue encountered in clinical settings is device-related infections; for example, catheter-associated infections, which are major causes of nosocomial bloodstream infections (32). Additionally, multi-drug resistance often occurs once biofilms mature; this problem may be compounded in polymicrobial biofilms, complicating treatment (33, 34).

An approach to managing biofilm infections is to control early stage surface colonization. Factors that affect surface colonization by microorganisms include electrical charge (35), hydrophobicity (36) and fimbriae (37). To date, limited work has been carried out on parameters affecting surface colonization by more than one strain of bacterium, especially in the presence of

multiple antibiotics as are used in combination therapies (38). In this work, we investigated factors affecting bacterial surface colonization in the presence of multiple antibiotics. These factors include 1) areal density, or the number of surface-attached cells during early stages of biofilm formation; 2) availability of nutrients during early attachment and its ultimate impact on biomass accumulation in the presence of antibiotics; and 3) how antibiotic exposure during initial biofilm formation impacts overall biofilm development in the presence of antibiotics. The work expands on a previously established method of constructing multi-species biofilms (39) and research on the role of antibiotic resistance mechanisms and biofilm structure on biofilm formation by antibiotic-sensitive and -resistant strains (40).

## 2.2 Materials and Methods

### 2.2.1 Strains and culture conditions

Strains were graciously provided by H.A. O'Connell and were handled as previously described (41). An antibiotic resistant strain of *Escherichia coli* ATCC 33456 harboring ampicillin resistance (Amp<sup>R</sup>) on a pUC19-based vector, pEGFP (Invitrogen, Carlsbad, CA) was used in this study. The pEGFP plasmid carries a gene for the green fluorescent protein (GFP) and a second gene coding for beta-lactamase (*bla*) which provides resistance to the antibiotic ampicillin. A second strain of *E. coli*, ATCC 33456 harboring spectinomycin resistance (Spec<sup>R</sup>) on a pUC18-based vector, pUCSpec, was also used. The pUCSpec plasmid provides resistance to the antibiotic spectinomycin. Both plasmids are from the same incompatibility group which reduces the chance of a single cell holding both plasmids. All inocula were prepared from stock cultures stored at -80°C. The *E. coli* Amp<sup>R</sup> strain was maintained on Luria-Bertani (LB) agar containing 400 ppm ampicillin, and the *E. coli* Spec<sup>R</sup> strain was maintained on LB agar containing 100 ppm

spectinomycin. Both strains were cultured overnight (18-19 h) at 37°C prior to use. Ampicillin and spectinomycin stocks were obtained from Sigma-Aldrich, Inc. (St. Louis, MO)

To prepare an inoculum, several loopfuls of each *E. coli* strain were aseptically transferred from each plate to their own 1 ml of sterile 50 mM phosphate buffer (pH 7.2). Cells were resuspended by vortexing and pipetting. The optical density at 600 nm (OD<sub>600</sub>) of each overnight suspension was measured by spectrophotometer (Pharmacia Biotech, New York, NY) and diluted to achieve a 5:1 ratio of *E. coli* Spec<sup>R</sup> to *E. coli* Amp<sup>R</sup> as previously described (39). After obtaining the desired optical density for the experiment, the combined inoculum was transferred into 100 ml of phosphate buffer or LB broth.

### **2.2.2 Cultivation of biofilms**

Flow-cell cultivation of biofilms was performed according to previously described methods (42). Each strain was recirculated (attachment phase) through flow cells (46 × 4 × 2 mm) alone or as co-cultures for 2 h in 50 mM phosphate buffer (pH 7.2) or LB broth at a flow rate of 0.84 ml min<sup>-1</sup>. A 5:1 ratio of various areal densities was used for these experiments based on previously described methods (39). For experiments involving antibiotic challenge during recirculation, 80 ppm spectinomycin + 100 ppm ampicillin were supplemented in the recirculation media. Following each recirculation period, flow cells were rinsed with 50 mM phosphate buffer (pH 7.2) for 10 min. For microscopic analysis at 2 h, attached cells were stained with a 50 μM solution of the red nucleic acid stain Syto 59 (Invitrogen, USA) for 10 min. followed by an additional 5 min rinse using 50 mM phosphate buffer (pH 7.2). For 24 h biofilms, flow cells were re-attached and switched to a continuous phase, supplemented with LB with or without antibiotics (80 ppm spectinomycin + 100 ppm ampicillin) at a flow rate of 0.35 mL min<sup>-1</sup> for the duration of the experiment. Preparation for microscopic analysis after 24 h was the same as 2 h.

### ***2.2.3 Microscopy and image analysis***

Colonized flow cells were imaged using a Zeiss LSM 510 confocal laser scanning microscope (CLSM) (Carl Zeiss, Thornwood, NY) equipped with a Fluor 40× oil immersion lens. Fluorescent excitation occurred simultaneously at wavelengths of 488 and 523 nm. A minimum of four image stacks from each channel were taken at different locations throughout the flow cell, using a 1- $\mu\text{m}$   $z$ -step increment. All data points for every experiment were measured in duplicate or triplicate. Quantitative analysis of image stacks was performed using the statistical package COMSTAT (43). Biovolume is quantified as biomass volume divided by substratum area ( $\mu\text{m}^3/\mu\text{m}^2$ ). It provides an estimate of the biomass in the biofilm and thus it is generally referred to as biomass (43).

### ***2.2.4 Statistical analysis***

Initial mutualistic interactions were analyzed using an independent-samples Kruskal-Wallis test ( $\alpha=0.05$ ). Experiments of effects of areal density and antibiotic exposure were analyzed using a two-way analysis of variance (ANOVA) ( $\alpha=0.05$ ).

## 2.3 Results

### 2.3.1 *Community-dependent antibiotic tolerance and biofilm establishment*

In establishing our model for evaluating interactions leading to biofilm establishment under challenging conditions, we initially screened concentrations of antibiotics that were inhibitory and suitable for our experiments. Concentrations of 80 ppm spectinomycin and 100 ppm ampicillin were selected based on these preliminary experiments. To demonstrate these interactions, each *E. coli* strain was recirculated independently of the other as well as in combination for 2 h in phosphate buffer, allowing colonization of the flow cell. A ratio of 5:1 *E. coli* Spec<sup>R</sup> to *E. coli* Amp<sup>R</sup> was used, with an approximate areal density of 600 cells (combined) and 500 (Spec<sup>R</sup>) and 100 (Amp<sup>R</sup>) cells separately. Subsequently, the cells were grown in LB + antibiotics for 24 h and analyzed for biomass accumulation. CLSM and image analysis from 24 h biofilms indicated that combined cultures of each *E. coli* strains resulted in significantly greater biomass accumulation than each strain alone, in the presence of both antibiotics relative to untreated controls (Fig. 2.1A and B). These observations suggested that a favorable interaction between both strains in co-culture allowed for biofilm formation to occur in the presence of a dual antibiotic challenge.

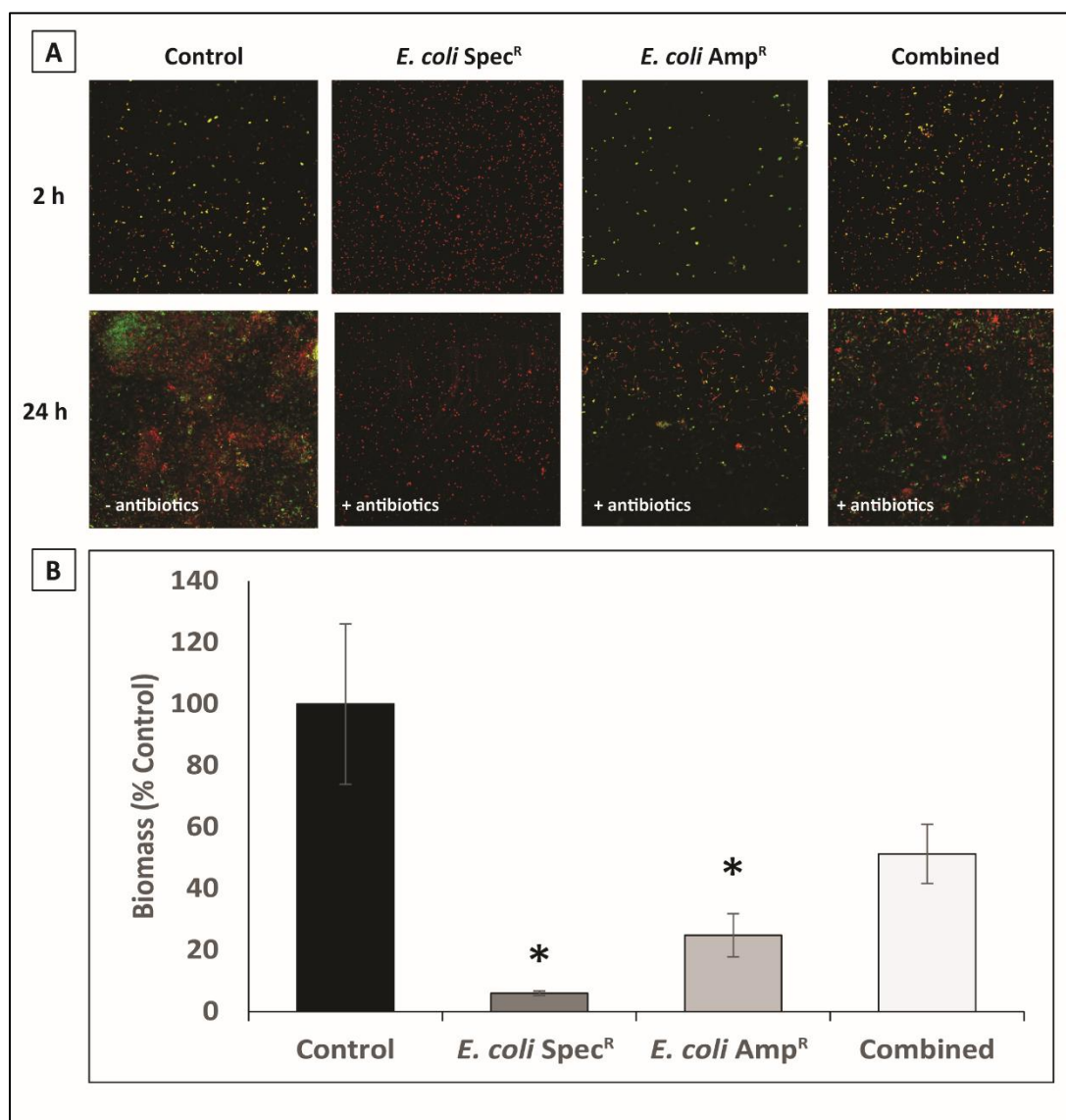


**Figure 2.1: Community-dependent biofilm establishment under antibiotic challenge.** (A) Top panel shows representative CLSM images of *E. coli* Spec<sup>R</sup> and *E. coli* Amp<sup>R</sup> alone and in co-cultures, recirculated in phosphate buffer for 2 h. *E. coli* Spec<sup>R</sup> appears red due to nucleic acid stain Syto 59, *E. coli* Amp<sup>R</sup> appears green due to ampicillin-induced expression of green fluorescent protein (GFP). Bottom panel represents growth condition in LB ( $\pm$  antibiotics) after 24 h. (B) The image analysis software package COMSTAT was used for biomass determination and all conditions were normalized to untreated controls. Values for each condition are means  $\pm$  standard error of the means for 2-3 replicates of each condition. An independent-samples Kruskal-Wallis test indicated a significant effect of culture condition ( $\chi^2(2) = 9.293$ ,  $p < 0.05$ ) at 24 h. Asterisks indicate that mean rank values of *E. coli* Spec<sup>R</sup> and *E. coli* Amp<sup>R</sup> are significantly different from the combined culture and untreated controls.

### 2.3.2 *Effects of areal density and antibiotic exposure on biofilm formation under antibiotic challenge: phosphate-recirculated cells*

We hypothesized that three factors during recirculation (attachment) contributed to biofilm growth by both *E. coli* strains in the presence of two inhibitory antibiotic concentrations, as seen in Figure 2.1. These factors were areal density, the presence or absence of antibiotics, and the presence or absence of nutrients. To determine the effect of areal density on biofilm growth, co-cultured inocula of *E. coli* Spec<sup>R</sup> and *E. coli* Amp<sup>R</sup> were recirculated for 2 h in phosphate buffer in the presence or absence of 80 ppm spectinomycin and 100 ppm ampicillin. The areal cell densities selected for these experiments were 600, 900, and 1200 cells per microscopic field, corresponding to x, y, and z cells mm<sup>-2</sup> respectively. Additionally, based on optimal conditions in previous findings (39) a 5:1 ratio of *E. coli* Spec<sup>R</sup> to *E. coli* Amp<sup>R</sup> was maintained with all experiments. After the 2 h recirculation phase, attached cells were irrigated for 24 h with either LB or LB supplemented with antibiotics (80 ppm spectinomycin + 100 ppm ampicillin). CLSM and image analysis indicated no significant main effects of areal density or antibiotic exposure (during recirculation) on biofilm biomass accumulation after 24 h, relative to controls ( $p > 0.05$ ; Fig. 2.2 A and B). This suggests that regardless of the areal density tested, using a 5:1 ratio at each one was sufficient in overcoming any adverse effects of antibiotic exposure during attachment and the 24 h period of biofilm development under antibiotic challenge. This may further suggest that the importance of the community-dependent interactions that occur under challenging conditions lies in the composition of the members of the biofilm community and their proximity to one another.

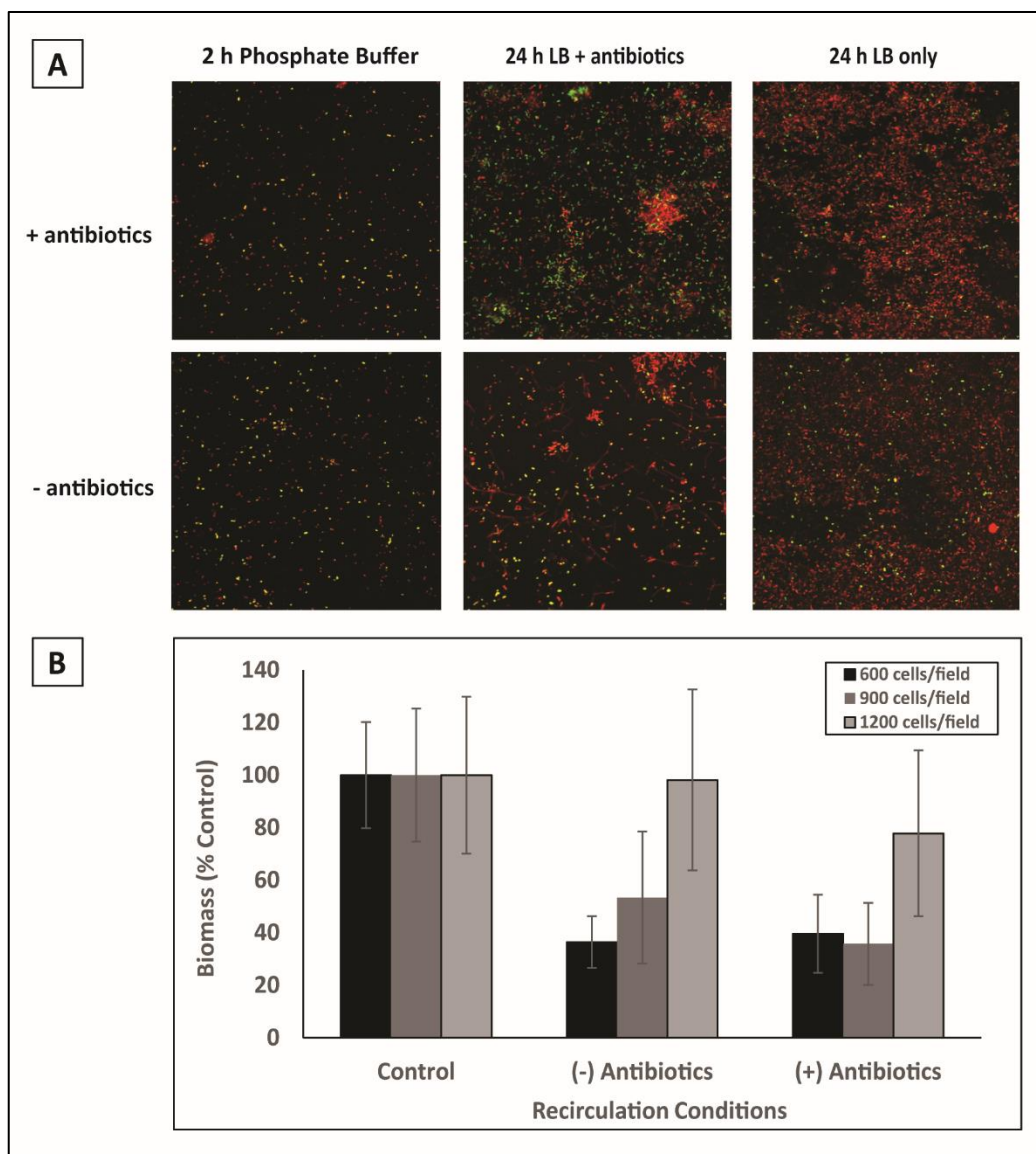


**Figure 2.2: Effects of areal density and antibiotic exposure on phosphate-recirculated cells in 24 h biofilm formation.** (A) Top panel shows representative CLSM images of *E. coli* Spec<sup>R</sup> and *E. coli* Amp<sup>R</sup> co-cultures at a 5:1 ratio (~1200 cells), recirculated in phosphate buffer (+ antibiotics) for 2 h and grown in LB ( $\pm$  antibiotics) for 24 h. Bottom panel is the same, except cells were recirculated in phosphate buffer (-antibiotics). *E. coli* Spec<sup>R</sup> appears red due to nucleic acid stain Syto 59, *E. coli* Amp<sup>R</sup> appears green due to ampicillin-induced expression of green fluorescent protein (GFP). (B) The image analysis software package COMSTAT was used for biomass determination and all conditions were normalized to untreated controls. Values for each condition are means  $\pm$  standard error of the means for 3 replicates of each condition. Two-way ANOVA indicated no significant main effects of either areal density or recirculation conditions. In addition, no significant interaction between areal density and recirculation conditions was determined.

### ***2.3.3 Effects of areal density and antibiotic exposure on biofilm formation under antibiotic challenge: LB-recirculated cells***

To determine whether the presence of nutrients during attachment impacted biofilm formation, co-cultures of *E. coli* Spec<sup>R</sup> and *E. coli* Amp<sup>R</sup> were grown as described in Section 2.3.2 except that LB broth was provided during the 2 h recirculation. CLSM and image analysis indicated a significant main effect of recirculation conditions ( $p < 0.05$ ), but no significant effect of areal density ( $p > 0.05$ ). These data indicated that there was a significant difference in untreated controls (no antibiotics at 2 and 24 h) and those that were recirculated in the presence or absence of antibiotics, followed by a 24 h antibiotic challenge (Fig. 2.3 A and B). Nutrient availability during the attachment phase, coupled with antibiotic exposure, did not appear to enhance antibiotic tolerance during the following 24 h growth, relative to co-cultures recirculated in the absence of antibiotics. Although nutrient availability during the attachment phase generally results in greater overall biomass, it does not necessarily result in a significant advantage during biofilm development under antibiotic challenge.

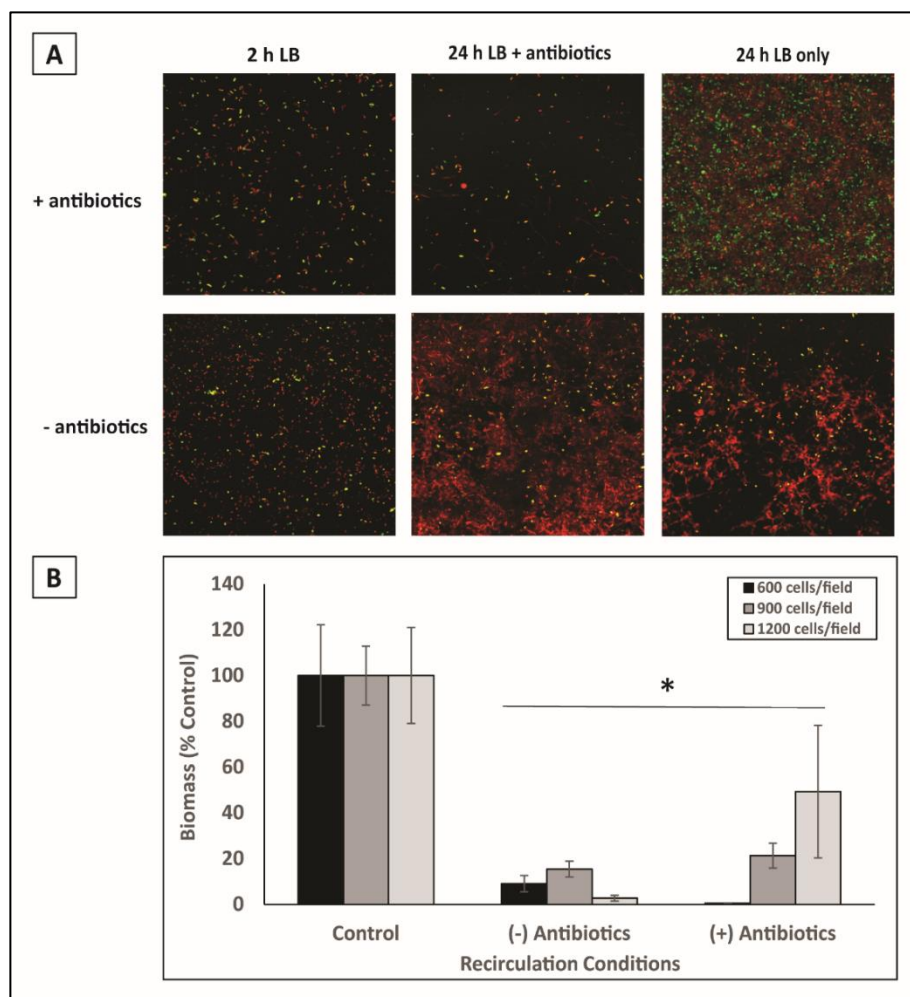


**Figure 2.3: Effects of areal density and antibiotic exposure on LB-recirculated cells in 24 h biofilm formation.** (A) Top panel shows representative CLSM images of *E. coli* Spec<sup>R</sup> and *E. coli* Amp<sup>R</sup> co-cultures at a 5:1 ratio (~1200 cells), recirculated in LB (+ antibiotics) for 2 h and grown in LB (± antibiotics) for 24 h. Bottom panel is the same, except cells were recirculated in LB (-antibiotics). *E. coli* Spec<sup>R</sup> appears red due to nucleic acid stain Syto 59, *E. coli* Amp<sup>R</sup> appears green due to ampicillin-induced expression of green fluorescent protein (GFP). (B) The image analysis software package COMSTAT was used for biomass determination and all conditions were normalized to untreated controls. Values for each condition are means ± standard error of the means for 3 replicates of each condition. Two-way ANOVA indicated no significant effect of the areal density factor ( $F_{[2, 96]} = 0.190$ ,  $p > 0.05$ ), but a significant main effect of recirculation condition ( $F_{[2, 96]} = 13.99$ ,  $p < 0.05$ ); *post hoc* tests show that untreated controls (no antibiotics at 2 and 24 h) were significantly different from cells recirculated with or without antibiotics at 2 h but challenged with antibiotics for 24 h ( $p < 0.05$ ). No significant interaction between areal density and recirculation conditions was determined ( $F_{[4, 96]} = 0.295$ ,  $p > 0.05$ ).

## 2.4 Discussion

The conditions present during substratum colonization are important factors in biofilm formation, particularly in the presence of multiple antibiotics. The biofilm structure is inherently resistant to biocidal treatments (5) and creates treatment hurdles that are further compounded by the presence of antibiotic resistant populations within the biofilm community. Community-dependent antibiotic resistance allows for multiple members of a microbial community, each harboring a unique antibiotic resistance gene, to coexist in close proximity in the presence of inhibitory concentrations of antibiotics. In evaluating these ecological interactions, it was determined that the ability of antibiotic resistant co-cultures to establish biofilms under antibiotic challenge occurred independently of areal density (i.e. number of attached cells during recirculation). We suspect that the alleviation of the effects of antibiotic exposure is related to two factors. This first is the proximity of each resistant cell type to one another, which facilitates the likelihood of a mutual antibiotic detoxification event to take place. These types of interactions were similarly observed by O'Connell and colleagues (40). The second factor is initiation of a stringent response simulated by recirculation in phosphate buffer. The stringent response is a low-nutrient stress response, which among others things, has been shown to regulate biofilm formation in *E. coli* (44, 45). Phosphate-recirculated cells experience a period of starvation during the attachment phase that may serve as an environmental trigger towards biofilm formation. This occurs regardless of antibiotic exposure during the same period. Once cells were switched over to a growth medium, biomass accumulation remains similar among all conditions after 24 h, perhaps due to a slower growth rate of the cells in the biofilm as well as residual effects of the antibiotics. It should also be noted that phosphate-recirculated cells grown in LB + antibiotics for longer periods (~ 48 h) resulted in greater biomass accumulation (39), suggesting that even in the presence

of an antibiotic challenge, given enough time, cooperative antibiotic detoxification will occur resulted in greater biomass.

In contrast to the nutrient-poor conditions modeled during phosphate recirculation, nutrient-rich conditions (LB) during the attachment phase generally resulted in increased biomass accumulation after 24 h. This was not totally unexpected since nutrient availability during the attachment phase would lead to rapid cell division and ultimately greater biomass accumulation after 24 h, when compared to phosphate-recirculated cells. However, the presence or absence of antibiotics during recirculation did not significantly help or hinder biofilm formation (24 h) under antibiotic challenge. Initially it was hypothesized that antibiotic exposure during the attachment phase might enhance biofilm formation by acting as an environmental cue, triggering cells to enter into the more protective biofilm phenotype. This type of reaction to inhibitory concentrations of antibiotics has been previously documented in both *E. coli* and *P. aeruginosa* and is linked to secondary messenger systems like cyclic-di-GMP (27). However, these findings seem to indicate that under nutrient-rich conditions the cells exposed to antibiotics do not fare any better than their counterparts which go unchallenged during attachment. Nutrient availability, in fact, may actually serve as a disadvantage to cells that experience antibiotic challenge. As it turns out, one of the key characteristics that allows members of a biofilm to resist antimicrobial treatments is reduced metabolic activity (46). Interestingly, Barraud *et al.* (47) similarly described how exposure to mannitol enhanced the metabolic activity of *P. aeruginosa* biofilm cells and subsequently enhanced their susceptibility to antibiotic treatment.

Although certain patterns were observed in our analysis of parameters like areal density and antibiotic exposure, these patterns did not reveal any discernable significance within the scope of our model. However, modifications to future experiments may help shed further light on the

interplay between these factors. Additionally, nutrient availability, antibiotic exposure, and areal density are certainly factors of clinical relevance when considering the ecological interactions that occur in chronic infections caused by biofilms; however, one should also consider these parameters when considering the use of biofilms as industrial catalyst. Conditions that initiate or promote biofilm formation could be essential in biofilm reactor design and ultimately yield of final products or removal of wastes (48).

The highlight of this method lies in its simplicity and reproducibility. The ability to construct *in vitro* models of microbial biofilms of both clinical and industrial relevance can help bridge the gap between bench-scale investigations and the ultimate application of therapeutic strategies and full-scale industrial applications.

*Santiago AJ, Ahmed MNA, Wang S-L, Damera K, Wang B, Tai PC, Gilbert ES, Derby CD.*

2016. Inhibition and Dispersal of *Pseudomonas aeruginosa* Biofilms by Combination Treatment with Escapin Intermediate Products and Hydrogen Peroxide. *Antimicrobial Agents and Chemotherapy* **60**:5554-5562.

Copyright © 2016, American Society for Microbiology

### **3 Inhibition and dispersal of *Pseudomonas aeruginosa* biofilms by combination treated of Escapin intermediate products and hydrogen peroxide.**

#### **3.1 Introduction**

In their natural environments, microorganisms most frequently exist as biofilms, or communities of microorganisms attached to surfaces and encased in a self-produced extracellular matrix (29). The properties of this matrix afford these microorganisms protection from environmental challenges including nutritional starvation and chemical treatments such as antibiotics. Biofilms have a well-documented impact in both industrial and clinical settings. In microbial infections, the protective and recalcitrant nature of the biofilm state leads to problems with treatment and clearance. Biofilms on medical devices such as catheters or implants can result in chronic infections that are resistant to therapeutic drugs (49, 50). Nosocomial infections, often associated with biofilm formation on medical devices or wound sites, contribute to higher morbidity and mortality rates as well as increased healthcare costs (50, 51). Industries such as wastewater treatment as well as food and agriculture are heavily impacted by the adverse effects of biofilms as well (52, 53). Consequently, the search for effective anti-biofilm strategies is an ongoing quest that looks to both natural and synthetic agents that are capable of preventing, disrupting, or eradicating biofilms, while reducing selective pressures that contribute to resistance.

An effective antimicrobial agent against planktonic microbes has been found in the ink of the marine gastropod mollusc *Aplysia californica* (sea hare) (54). The ink is the product of two simultaneously released glandular secretions; upon attack by predators, the sea hare releases both products into the mantle cavity where they are mixed before being ejected from the animal (55, 56). One of the bioactive ingredients in the secretion is Escapin, an L-amino acid oxidase (25). Escapin and its major natural substrate, L-lysine, are secreted at nearly 2 mg/ml and 150 mM respectively (57-59). A series of Escapin-catalyzed and non-enzymatic chemical reactions yields an equilibrium mixture of a diverse set of molecules referred to as Escapin intermediate products (EIP), which can be synthesized and are effective as naturally produced products (Fig. 3.1) (1, 60). Hydrogen peroxide ( $H_2O_2$ ) and ammonium are also produced. The equilibrium among the components of EIP is dependent on pH, with the cyclic form, compound 3, dominating at any pH.

The combination of EIP and  $H_2O_2$ , annotated as “EIP +  $H_2O_2$ ” throughout this work, is bactericidal against a wide range of planktonic microbes including Gram-negative and Gram-positive bacteria, yeast, and fungi (1, 25). At low millimolar concentrations, EIP +  $H_2O_2$  produces rapid, powerful, and long lasting bactericidal activity against planktonic cells, probably through condensation of DNA (1, 28). EIP +  $H_2O_2$  is an especially effective agent against planktonic cultures of *P. aeruginosa* (1). Given the bactericidal effects of EIP +  $H_2O_2$  against planktonic bacteria, and in particular *P. aeruginosa*, we focused on the effectiveness of EIP +  $H_2O_2$  against bacterial biofilms. *P. aeruginosa* is a well-known opportunistic pathogen whose biofilms cause chronic infections, morbidity, and mortality (61-63). Taking into account the effectiveness of EIP +  $H_2O_2$  against this bacterium (1) and its clinical relevance as a formidable pathogen, the objective of this study was to determine the effectiveness of EIP +  $H_2O_2$  in preventing the formation of and disrupting existing biofilms of *P. aeruginosa*.

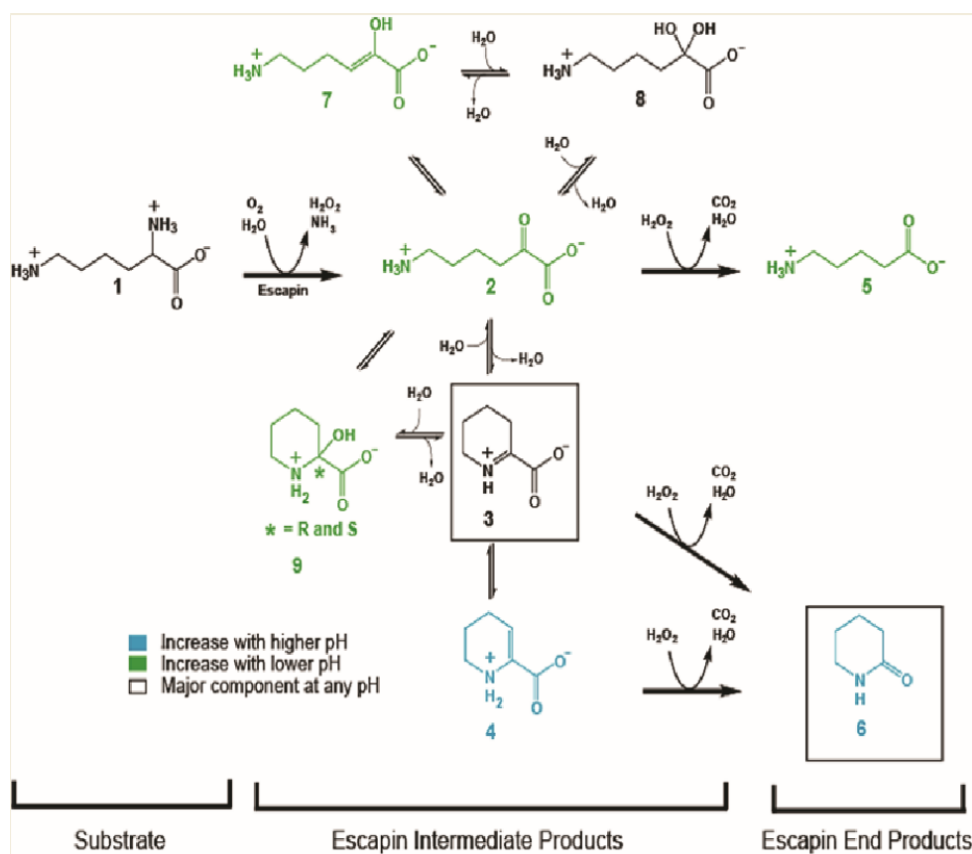


**Figure 3.1: Summary of the chemistry of the reaction of Escapin with L-lysine, including the effects of pH on the relative composition of the molecular species in the equilibrium mixture.** Figure reprinted with permission from Ko *et al.* 2008 (1). Compounds are: L-lysine (compound 1),  $\alpha$ -keto- $\epsilon$ -aminocaproic acid (compound 2),  $\Delta^1$ -piperidine-2-carboxylic acid (compound 3),  $\Delta^2$ -piperidine-2-carboxylic acid (compound 4),  $\gamma$ -aminovaleric acid (compound 5),  $\gamma$ -valerolactam (compound 6), 6-amino-2-hydroxy-hex-2-enoic acid (compound 7), 6-amino-2,2-dihydroxy-hexanoic acid (compound 8), and 2-hydroxy-piperidine-2-carboxylic acid (compound 9).

## 3.2 Materials and Methods

### 3.2.1 Culture preparation

*Pseudomonas aeruginosa* PAO1 was grown in *Pseudomonas* Basal Mineral Medium, supplemented with glucose (80 mM final concentration) (PBM-glucose) (64) at 37 °C with shaking at 200 rpm for 16-18 h. Frozen stocks (10% glycerol/-80 °C) were thawed and 35  $\mu$ l were added

to 30 ml of PBM-glucose in a 50 ml flask. Overnight cultures were diluted with fresh PBM-glucose to obtain initial inoculum densities of  $OD_{600} = 0.01$  or  $0.10$  for biofilm formation and dispersal assays, respectively.

### 3.2.2 Chemicals

Escapin intermediate products (EIP) was synthesized as described in Kamio *et al.* (60) based on Lu and Lewin (65) using a non-enzymatic synthesis starting with pipercolinic acid ethyl ester.  $\Delta^1$ -Piperidine-2-carboxylic acid (compound 3) is the major product and  $\Delta^2$ -piperidine-2-carboxylic acid (compound 4) is the minor product of this synthesis, though in solution, compounds 3 and 4 form an equilibrium mixture with other compounds, as shown in Figure 3-1. The preparation of EIP used in each treatment is derived from the synthetic preparation of  $\Delta^1$ -piperidine-2-carboxylic acid and used as the initial molecule to generate the EIP equilibrium mixture. This synthesis allows for the independently controlled presentation of these two major components of Escapin's products, EIP and  $H_2O_2$ . Freeze-dried EIP was stored at  $-80\text{ }^\circ\text{C}$  and dissolved in sterile deionized (DI) water as a 1 M stock and diluted at the time of experiment. Hydrogen peroxide ( $H_2O_2$ , 30%) was purchased from Fisher Scientific (Cat. No. H325-100). For experiments, treatment concentrations of EIP and  $H_2O_2$  were prepared in *Pseudomonas* Basal Mineral Medium without glucose (PBM-no glucose) in order to prevent further growth during treatment periods.

Live/Dead<sup>®</sup> BacLight<sup>™</sup> Bacterial Viability Kit (L-7012) was purchased from Life Technologies (CA, USA). This kit includes two different nucleic acid stains: SYTO 9<sup>®</sup> and propidium iodide (PI). SYTO 9<sup>®</sup> is a green-fluorescent dye that labels bacteria with either intact or damaged membranes. PI is a red-fluorescent dye that can only penetrate bacteria with damaged membranes and that reduces SYTO 9<sup>®</sup> fluorescence when both dyes are present.

### **3.2.3 Assay of biofilm formation**

Biofilms were cultured in 96-well polystyrene microtiter plates (20, 66, 67) using PBM-glucose as the growth medium. Briefly, biofilms were grown for 5 h (attachment phase) in the presence of EIP + H<sub>2</sub>O<sub>2</sub>, EIP alone, H<sub>2</sub>O<sub>2</sub> alone, and PBM-glucose alone as the control. After incubation and treatment periods, biofilms were rinsed with sterile, deionized (DI) water by consecutively submerging microtiter plates in three separate tubs for 10 sec each, followed by shaking out extra water. The biofilms were stained with 125 µl of 0.02% crystal violet (125 µl 0.3% crystal violet (Becton Dickinson, NJ) in 2 ml DI water) for 15 min at room temperature with shaking at 200 rpm. After staining, 96-well plates were rinsed with DI water three times. Plates were allowed to air dry for a minimum of 1 h or overnight. For quantification, bound crystal violet was dissolved with 125 µl of 95% ethanol for 30 min at room temperature with shaking at 200 rpm. Absorbance of dissolved crystal violet was measured by spectrophotometer at 570 nm using 95% ethanol as the blank. Treatment conditions were normalized to untreated controls and biofilm inhibition, as determined by biomass accumulation, is expressed as biomass (% control).

### **3.2.4 Assay of biofilm dispersal**

Biofilms were grown in flow cells as described previously (20, 42, 68) using PBM-glucose as the growth medium. Frozen stocks of strain PAO1 were inoculated (35 µl added to 30 ml medium) into PBM-glucose in a 50 ml flask and incubated at 37 °C with shaking at 200 rpm for 16-18 h. The overnight culture was diluted with fresh PBM-glucose to obtain an OD<sub>600</sub> of 0.10. Biofilms were grown in flow cells for 20 h in recirculation mode and were rinsed for 20 min with PBM-no glucose (rinse buffer). Biofilms were then treated with EIP + H<sub>2</sub>O<sub>2</sub>, EIP alone, H<sub>2</sub>O<sub>2</sub> alone, or a PBM-no glucose control for 30 min followed by a 10 min rinse with PBM-no glucose prior to staining. One ml of a staining solution consisting of LIVE/DEAD<sup>®</sup> BacLight<sup>™</sup> Bacterial

Viability Kit (3.34  $\mu\text{M}$  SYTO 9 and 20  $\mu\text{M}$  propidium iodide) was used to stain the biofilm for 15 min, followed by a 5 min rinse with PBM-no glucose. Microscopic imaging of each flow cell was performed using a Zeiss LSM 510 confocal laser-scanning microscope (Carl Zeiss, Thornwood, NY). A minimum of 10 image stacks with a 1  $\mu\text{m}$  z-step were taken for each channel of the flow cell using a 40 $\times$  oil immersion lens. The excitation/emission wavelengths of 480/500 nm and 490/635 nm were used for SYTO 9 and propidium iodide, respectively, using argon and helium-neon (HeNe) lasers. Quantitative analysis of image stacks was performed using the statistical package COMSTAT (43). Biovolume is quantified as biomass volume divided by substratum area ( $\mu\text{m}^3/\mu\text{m}^2$ ). It provides an estimate of the biomass in the biofilm and thus it is generally referred to as biomass (43). Area layer is the fraction of the area occupied by biomass (%) in each image of a stack (i.e. distance from the substratum ( $\mu\text{m}$ )) (43). Image stacks are 1  $\mu\text{m}$  slice images that are stacked by the CLSM program to generate a three dimensional image of the biofilm. Area layer analysis determines what fraction of each 1- $\mu\text{m}$  slice is occupied by biomass from the substratum to the apex of the biofilm.

### **3.2.5 Motility assays**

Motility assays were performed as described previously (69, 70) with some modification. Media used for the assay was Luria-Bertani (LB) broth, Miller (Difco) (tryptone 10 g/l, yeast extract 5 g/l, sodium chloride 10 g/l) (Fisher Scientific Cat. No. DF0446-07-5) containing 0.3% (wt/vol) Bacto agar (Fisher Scientific Cat. No. DF0140-15-4) for swimming, 0.5% (wt/vol) Bacto agar for swarming, and 1% (wt/vol) for twitching plates. For initial screens of effects of EIP on motility, 10  $\mu\text{l}$  of either PBM-no glucose (control) or various concentrations of EIP (50, 100, 200, 400, 800, 1000  $\mu\text{M}$ ) (treatment) were spotted at the center of each corresponding motility plate and allowed to dry for approximately 5-10 min prior to inoculating bacteria. In subsequent

swimming motility experiments, EIP (50  $\mu\text{M}$  or 100  $\mu\text{M}$ ),  $\text{H}_2\text{O}_2$  (3  $\mu\text{M}$  or 6  $\mu\text{M}$ ), or EIP +  $\text{H}_2\text{O}_2$  (3  $\mu\text{M}$   $\text{H}_2\text{O}_2$  + 50  $\mu\text{M}$  EIP or 6  $\mu\text{M}$   $\text{H}_2\text{O}_2$  + 100  $\mu\text{M}$  EIP) were applied to each plate in the same manner. To account for the single 10  $\mu\text{l}$  application of EIP and  $\text{H}_2\text{O}_2$ , as compared to the constant flow presented in flow cell treatments, higher concentrations of each compound were tested, also taking into account diffusion of the compound through the agar matrix as well as the possibility of chemical instability. Swimming and swarming plates were gently inoculated at the agar surface at the center of each plate with bacteria from an overnight culture streaked on LB agar plates (1.5% wt/vol) using sterile toothpicks. Twitching plates were inoculated by stabbing the toothpick through the agar at the center of each plate, making sure to make contact with the bottom surface of the plate. Plates were sealed with Parafilm to prevent dehydration and incubated at 37°C for 24 h. The diameter (measured in mm) of the motility zone was measured at intervals of 2, 4, and 24 h and used to determine the area ( $\text{mm}^2$ ) of the zone. Treatments were normalized to the mean values for each replicate of the untreated controls and motility zones are expressed as area (% control).

### **3.2.6 Statistical analysis**

Prevention of biofilm formation was analyzed using two-way analysis of variance (ANOVA) ( $\alpha=0.05$ ). Analysis of biofilm dispersal and undamaged/damaged ratios were done using one-way ANOVA ( $\alpha=0.05$ ). A repeated measures ANOVA ( $\alpha=0.05$ ) was used in analyzing area layer data. Motility experiments were analyzed using an independent-samples  $t$  test ( $\alpha=0.05$ ) and independent-samples Kruskal-Wallis test ( $\alpha=0.05$ ).

### 3.3 Results

#### 3.3.1 *EIP + H<sub>2</sub>O<sub>2</sub> in combination inhibit P. aeruginosa biofilm formation at micromolar concentrations*

Preliminary data collected to determine effective concentrations of EIP and H<sub>2</sub>O<sub>2</sub> for biofilm prevention studies indicated that micromolar concentrations of both EIP and H<sub>2</sub>O<sub>2</sub> were of particular interest. To examine these conditions further, *P. aeruginosa* was grown in microtiter plates for 5 h, simulating the attachment phase of the biofilm life cycle, in the presence of varying concentrations of H<sub>2</sub>O<sub>2</sub> alone, EIP alone, or EIP + H<sub>2</sub>O<sub>2</sub> (Fig. 3.2). H<sub>2</sub>O<sub>2</sub> alone resulted in reduced biofilm formation, particularly at the concentrations of 48 μM and 96 μM which resulted in an approximate 44% and 30% reduction in biomass, respectively, relative to untreated controls. EIP alone, at either 3 μM or 30 μM, resulted in 25% and 17% less biofilm formation respectively, compared to untreated controls. EIP + H<sub>2</sub>O<sub>2</sub>, at H<sub>2</sub>O<sub>2</sub> concentrations ≥ 24 μM, resulted in up to 47% less biofilm formation relative to untreated controls. The greatest effect on biofilm formation was observed when EIP was paired with 96 μM H<sub>2</sub>O<sub>2</sub>, resulting in more than 65% less biofilm formation, relative to untreated controls. Two-way ANOVA indicated a significant treatment effect (H<sub>2</sub>O<sub>2</sub>, 3 μM EIP + H<sub>2</sub>O<sub>2</sub>, 30 μM EIP + H<sub>2</sub>O<sub>2</sub>) and a significant concentration effect (H<sub>2</sub>O<sub>2</sub> at 0 to 96 μM) but a non-significant treatment-concentration interaction. *Post hoc* analysis of the treatment effect indicated that combination treatment of EIP (3 μM or 30 μM) + H<sub>2</sub>O<sub>2</sub> resulted in significantly less biofilm formation than single treatments. *Post hoc* analysis of the H<sub>2</sub>O<sub>2</sub> concentration effect showed that higher concentrations resulted in significantly less biofilm formation than lower concentrations. Thus, while EIP and H<sub>2</sub>O<sub>2</sub> alone only resulted in 20 to 30% less biofilm formation than the untreated controls, EIP (3 μM or 30 μM) + H<sub>2</sub>O<sub>2</sub> (96 μM) resulted in nearly 70% less biofilm formation than the control. The effects of EIP and H<sub>2</sub>O<sub>2</sub> were assessed

after 12 h to determine if inhibition of biofilm formation was maintained (data not shown). However, the inhibitory effects diminished over this period, most likely due to a reduction in the chemical stability of the EIP.

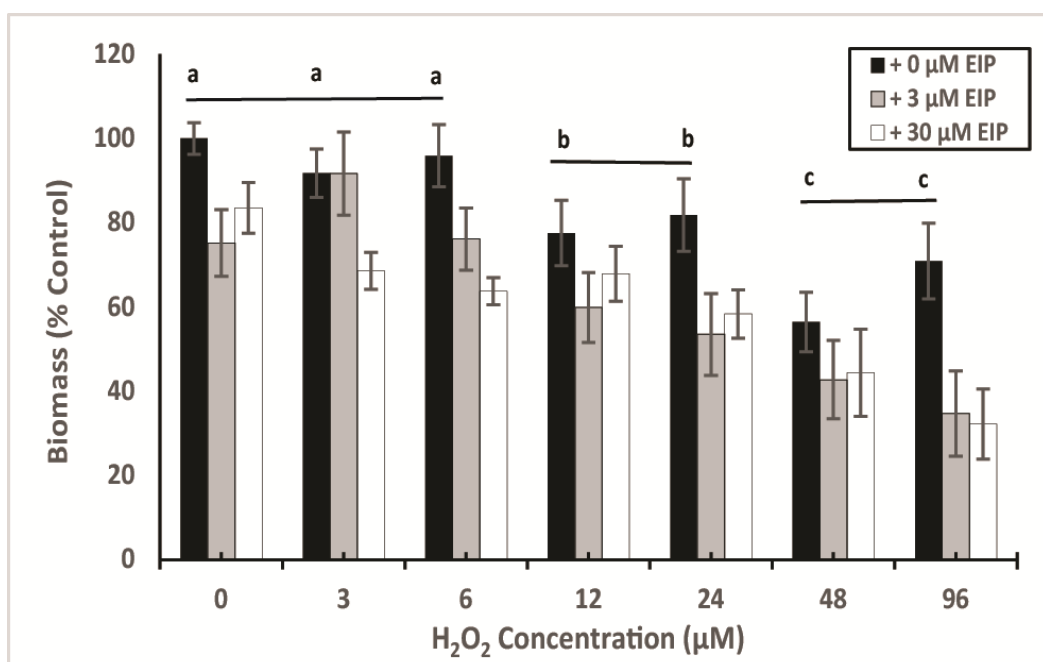


**Figure 3.2: Effects of EIP and H<sub>2</sub>O<sub>2</sub> on *P. aeruginosa* biofilm formation.**

*P. aeruginosa* biofilms were grown for 5 h in the presence of varying concentrations of: H<sub>2</sub>O<sub>2</sub> alone (black bars); 3 μM EIP alone or in combination with H<sub>2</sub>O<sub>2</sub> alone (gray bars); or 30 μM EIP alone or in combination with H<sub>2</sub>O<sub>2</sub> (white bars). Negative control (untreated) was PBM-glucose. Prevention of biofilm formation was determined by 96-well microtiter plate crystal violet assay. The values for each treatment including control (PBM-glucose) are means ± standard errors of the means for three replicates for each experimental condition. Total number of measurements for each treatment ranged from 23-48. Two-way ANOVA indicated a significant effect for the treatment factor ( $F_{[2,473]} = 18.57$ ,  $p < 0.05$ ); *post hoc* tests show that the H<sub>2</sub>O<sub>2</sub> alone treatment is significantly different from H<sub>2</sub>O<sub>2</sub> + 3 μM EIP and H<sub>2</sub>O<sub>2</sub> + 30 μM EIP ( $p < 0.05$ ). Additionally, a significant effect was determined for the H<sub>2</sub>O<sub>2</sub> concentration factor ( $F_{[6,473]} = 11.43$ ,  $p < 0.05$ ); *post hoc* tests show that the values for 0 μM = 3 μM = 6 μM (a) > 12 μM = 24 μM (b) > 48 μM = 96 μM (c). The interaction between the treatment factor and the H<sub>2</sub>O<sub>2</sub> concentration factor was not significant ( $F_{[12,473]} = 0.91$ ,  $p > 0.05$ ).

### 3.3.2 *EIP and H<sub>2</sub>O<sub>2</sub> work synergistically to disperse P. aeruginosa biofilms*

To examine the dispersal effects of EIP + H<sub>2</sub>O<sub>2</sub> on established biofilms, a range of concentrations of H<sub>2</sub>O<sub>2</sub> plus one concentration of EIP (50 μM) were tested using biofilms cultivated in flow cells for 20 h. Preliminary experiments (data not shown) indicated various EIP concentrations (above and below our treatment condition) that resulted in biofilm disruption; a concentration of 50 μM resulted in more pronounced disruption when paired with H<sub>2</sub>O<sub>2</sub> and thus was selected as the treatment concentration. Representative CLSM images of 20 h old biofilms treated with 3 μM H<sub>2</sub>O<sub>2</sub> alone, 3 μM H<sub>2</sub>O<sub>2</sub> + 50 μM EIP, and 50 μM EIP alone show the disruptive effects of the combined treatment versus H<sub>2</sub>O<sub>2</sub> or EIP alone (Fig. 3.3A). The combined treatment resulted in greater biomass clearance (indicated by black color (no cells)) and less stained biomass (yellow) compared to the control and other treatments (Fig. 3.3A). One-way ANOVA showed that combination treatments, including the combinations of 50 μM EIP plus either 0.03 μM H<sub>2</sub>O<sub>2</sub> or 3 μM H<sub>2</sub>O<sub>2</sub>, but not the respective single treatments, significantly reduced biofilm biomass, by 42% and 37% respectively, relative to control levels (Fig. 3.3B). Treatments with 30 μM and 300 μM H<sub>2</sub>O<sub>2</sub> alone, were not significantly different than their corresponding combined treatments with 50 μM EIP, suggesting a small window of concentrations ranges in which synergistic effects take place.

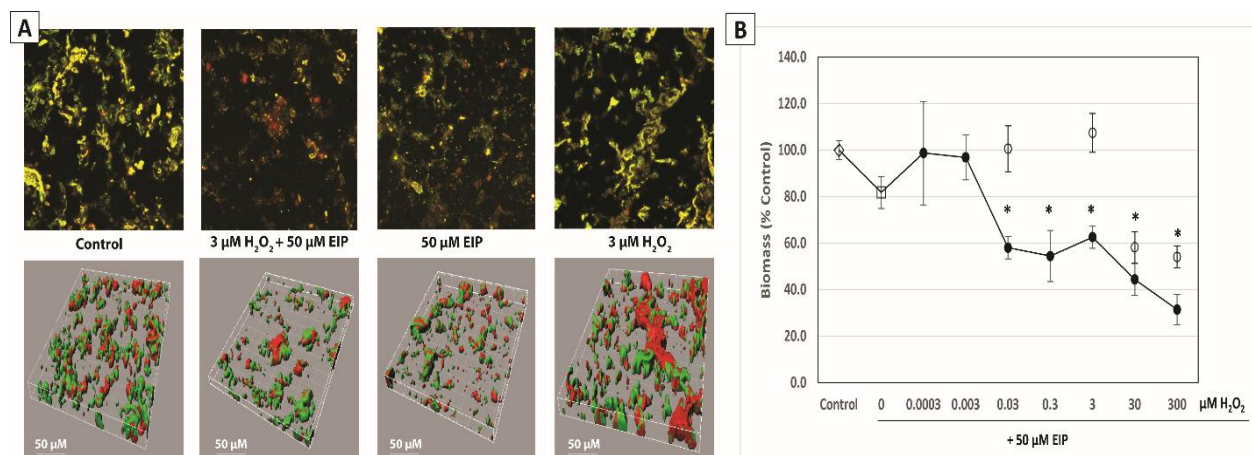


**Figure 3.3: Effects of EIP on *P. aeruginosa* and biofilm cell viability and biomass.**

Representative confocal microscopy images of 20 h *P. aeruginosa* biofilms following treatment with 3  $\mu\text{M}$   $\text{H}_2\text{O}_2$  alone, 50  $\mu\text{M}$  EIP alone, 3  $\mu\text{M}$   $\text{H}_2\text{O}_2$  + 50  $\mu\text{M}$  EIP, and control (PBM-no glucose). Shown is cell viability labeling using LIVE/DEAD® BacLight™ nucleic acid stain where green labeling represents live and undamaged cells, red labeling represents cells that are dead or with damaged membranes, yellow represents areas where green and red labeling are co-localized in the biofilm and black labeling represents area without cells. Bottom panel shows representative 3-dimensional projections of the representative confocal images. Scale bar, 50  $\mu\text{m}$ . (B) Effects of EIP +  $\text{H}_2\text{O}_2$  against *P. aeruginosa* biofilm (i.e. biofilm disruption). Flow-cell cultivated *P. aeruginosa* biofilms (20 h) were analyzed post-treatment by CLSM. The image analysis software package COMSTAT was used for biomass determination and all treatments were normalized to untreated controls. Open diamond is untreated control; open square is 50  $\mu\text{M}$  EIP alone; open circles are  $\text{H}_2\text{O}_2$  alone; closed circles are EIP +  $\text{H}_2\text{O}_2$ . Values are means  $\pm$  standard errors of the means for three replicates for each experimental condition. A range of 5 to 10 image stacks were taken for each biofilm; the total number of measurements for each treatment ranged from 4-172. ANOVA showed that the 7 treatments significantly differ in their effect on biofilm biomass ( $F_{[12,472]} = 8.21$ ,  $p < 0.05$ ), and *post hoc* tests show that EIP +  $\text{H}_2\text{O}_2$  but not EIP or  $\text{H}_2\text{O}_2$  is significantly different from the control ( $p < 0.01$ ). Asterisks indicate that the value of the EIP +  $\text{H}_2\text{O}_2$  at concentrations of 0.03  $\mu\text{M}$  or greater and  $\text{H}_2\text{O}_2$  alone at 30  $\mu\text{M}$  and 300  $\mu\text{M}$  is significantly lower than that of untreated control and EIP +  $\text{H}_2\text{O}_2$  at concentrations  $\leq 0.003$   $\mu\text{M}$ .

### 3.3.3 Treatment with EIP or EIP + $\text{H}_2\text{O}_2$ disperses but does not increase membrane damage within *P. aeruginosa* biofilm.

The ability of EIP +  $\text{H}_2\text{O}_2$  to cause membrane damage and impact viability of biofilm cells was assessed by measuring the ratio of green to red stained cells in biofilm images collected by CLSM. One-way ANOVA indicated that treatment with 3  $\mu\text{M}$   $\text{H}_2\text{O}_2$  + 50  $\mu\text{M}$  EIP or 50  $\mu\text{M}$  EIP alone significantly reduced biofilm biomass compared to untreated controls and treatments with 3

$\mu\text{M H}_2\text{O}_2$  alone (Fig. 3.4A). Measurements of green and red biomass from these treatments were used to determine a ratio of undamaged to damaged cells to determine the impact of treatment on membrane integrity (Fig. 3.4B). An undamaged/damaged ratio less than one is indicative of a greater presence of damaged cells. The undamaged/damaged ratios for all treatments, including the untreated control, were all greater than two, suggesting that the effects of the treatments did not result in increased membrane damage to the biofilm cells. The undamaged/damaged ratios for  $3 \mu\text{M H}_2\text{O}_2 + 50 \mu\text{M EIP}$  and  $3 \mu\text{M H}_2\text{O}_2$  were not significantly different from the untreated control, and the undamaged/damaged ratio for  $50 \mu\text{M EIP}$  was significantly greater than all other treatments. Taken together with our other results, these experiments support the idea that EIP and  $\text{H}_2\text{O}_2$  are dispersive, but not through a mechanism of membrane damage.

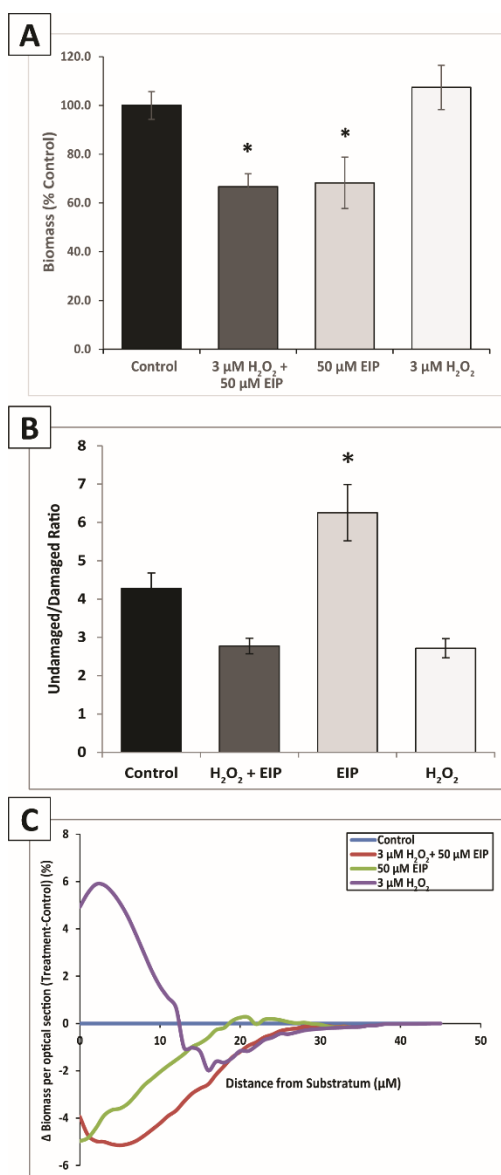


**Figure 3.4: Effects of EIP and  $\text{H}_2\text{O}_2$  on *P. aeruginosa* biofilm disruption.** (A) Flow-cell cultivated biofilms were analyzed post-treatment by CLSM. The image analysis software package COMSTAT was used for biomass determination and all treatments were normalized to untreated controls. Values are means  $\pm$  standard errors of the means for three replicates. Ten image stacks were taken for each biofilm; the total number of measurements for each treatment ranged from 30-109. ANOVA showed that two treatments significantly differ in their effect on biofilm biomass ( $F_{[3,205]} = 10.24$ ,  $p < 0.05$ ); *post hoc* tests show that 3  $\mu\text{M}$   $\text{H}_2\text{O}_2$  + 50  $\mu\text{M}$  EIP and 50  $\mu\text{M}$  EIP but not 3  $\mu\text{M}$   $\text{H}_2\text{O}_2$  are significantly different from the control ( $p < 0.05$ ). Asterisks indicate that the values for 3  $\mu\text{M}$   $\text{H}_2\text{O}_2$  + 50  $\mu\text{M}$  EIP and 50  $\mu\text{M}$  EIP are significantly lower than the values for the untreated controls and 3  $\mu\text{M}$   $\text{H}_2\text{O}_2$ . (B) Undamaged/damaged ratios were derived by dividing green biomass measurements by red biomass measurements. Treatments evaluated were 3  $\mu\text{M}$   $\text{H}_2\text{O}_2$ , 50  $\mu\text{M}$  EIP, 3  $\mu\text{M}$   $\text{H}_2\text{O}_2$  + 50  $\mu\text{M}$  EIP, and untreated controls. ANOVA showed that the undamaged/damaged ratio significantly differs across the treatments ( $F_{[3,233]} = 2951.10$ ,  $p < 0.05$ ); *post hoc* tests show that the undamaged/damaged ratio for 50  $\mu\text{M}$  EIP was significantly different from all other treatments ( $p < 0.05$ ). (C) Area layer was determined by COMSTAT analysis and is a measurement of the fraction of the area occupied by biomass (%) in each image of a stack (i.e. distance from the substratum ( $\mu\text{M}$ )). The differences in the mean area layer of biofilms in each treatment group relative to biofilms of untreated controls were used to determine how the biofilm structure (from substratum to apex) was affected by our treatments. A repeated measures ANOVA showed a significant effect on area layer by treatment condition; *post hoc* tests showed that treatments of 3  $\mu\text{M}$   $\text{H}_2\text{O}_2$  + 50  $\mu\text{M}$  EIP and 50  $\mu\text{M}$  EIP were significantly different than treatment with 3  $\mu\text{M}$   $\text{H}_2\text{O}_2$  alone.

### ***3.3.4 EIP and EIP + H<sub>2</sub>O<sub>2</sub> disrupt the biofilm structure from substratum to apex***

Comparison of biofilm biomass after treatment with H<sub>2</sub>O<sub>2</sub>, EIP, and EIP + H<sub>2</sub>O<sub>2</sub> revealed that the combination treatment of these compounds resulted in significant dispersal of *P. aeruginosa* biofilms, relative to untreated controls (Fig. 3.4A). To determine if EIP + H<sub>2</sub>O<sub>2</sub> affects the biomass distribution within the biofilm, the area layer function of COMSTAT was used to analyze CLSM-derived image stacks. Area layer measures the fraction of the area occupied by biomass (%) in each image of a stack as a function of distance from the substratum. By calculating the differences in the mean area layer of biofilms in each treatment group relative to biofilms of untreated controls, we determined how the biomass distribution within the biofilm was affected by the treatments (Fig. 3.4C). Treatment with 3 μM H<sub>2</sub>O<sub>2</sub> + 50 μM EIP or with 50 μM EIP led to a significant decrease in biomass from substratum to apex relative to the untreated controls. On the other hand, 3 μM H<sub>2</sub>O<sub>2</sub> alone caused biomass accumulation near the substratum relative to untreated controls.

### ***3.3.5 EIP and EIP + H<sub>2</sub>O<sub>2</sub> enhances P. aeruginosa swimming motility***

To determine if biofilm dispersal, in the absence of increased membrane damage, was mediated through a motility mechanism, a series of agar plate-based motility assays were performed to test the effects of EIP on swimming, swarming, and twitching motility. Initially, a concentration of 1 mM EIP was tested in order to account for the diffusion of the compounds through the agar matrix as well as compound stability over the duration of the assay. These preliminary experiments showed that exposure to 1 mM EIP did not enhance or inhibit swarming or twitching motility; however, swimming motility was significantly enhanced relative to untreated controls (data not shown). Subsequently, a series of EIP concentrations below 1 mM was tested (50, 100, 200, 400, 800 μM) to identify the range of effective treatment concentrations.

Motility was monitored over a period of 2 and 4 h to determine the duration of any effects. Exposure to 50  $\mu\text{M}$  EIP did not result in a significant increase in swimming motility relative to untreated controls (Fig. 3.5). However, only a 2-fold increase in concentration (100  $\mu\text{M}$  EIP) was required to significantly enhance swimming motility relative to untreated controls. This effect was observed over the course of 4 h (Fig. 3.5B). To determine the combined effects of EIP +  $\text{H}_2\text{O}_2$  on motility, concentrations used in biofilm dispersal assays (3  $\mu\text{M}$   $\text{H}_2\text{O}_2$  and 50  $\mu\text{M}$  EIP) were tested either alone or in combination, but they did not result in any enhancement in swimming motility over the course of 4 h (data not shown). However, by increasing the  $\text{H}_2\text{O}_2$  concentration 2-fold (6  $\mu\text{M}$ ), its combined effect with 100  $\mu\text{M}$  EIP enhanced *P. aeruginosa* swimming motility significantly (~80% after 2 h; ~40 % after 4 h), compared to each treatment alone and untreated controls (Fig. 3.6).

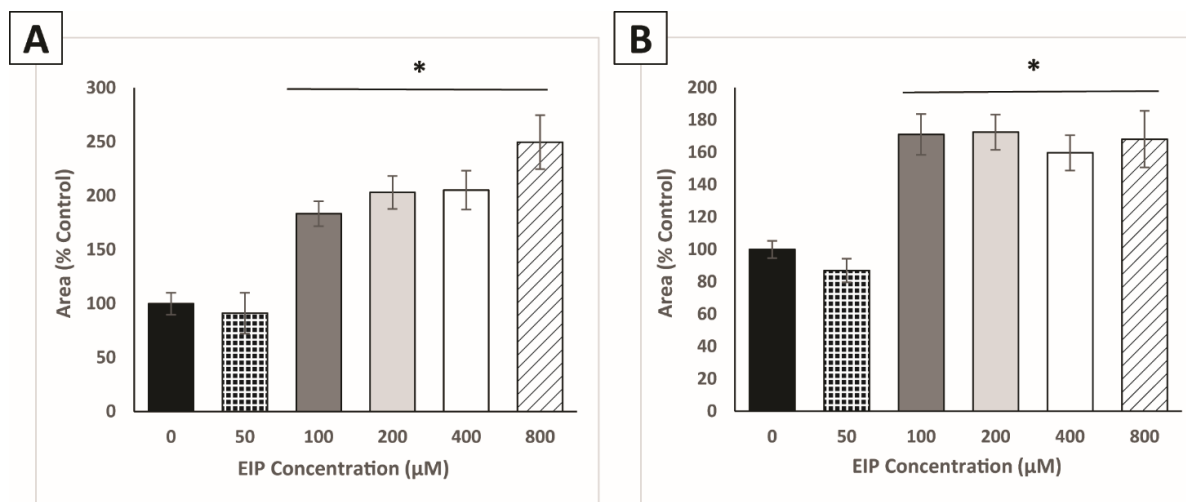


**Figure 3.5: Effects of EIP on motility at 2 and 4 h.** (A) Effects of 50, 100, 200, 400, and 800 µM EIP on *P. aeruginosa* swimming motility after 2 h at 37°C. Swimming motility for each treatment was quantified by measuring the diameter (mm) of each motility zone and calculating the area (mm<sup>2</sup>) of each zone after incubation. Treatments are as follows: untreated control (PBM-no glucose) (black bar), 50 µM EIP (checkered bar), 100 µM EIP (dark gray bar), 200 µM EIP (light gray bar), 400 µM EIP (white bar), and 800 µM EIP (diagonal bar). Values are means ± standard errors of the means for three replicates for each experimental condition. Treatments were normalized to untreated controls after taking the mean of the values for each of the control replicates. An independent-samples Kruskal-Wallis test indicated a significant effect of treatment on swimming motility ( $\chi^2(5) = 40.118$ ,  $p < 0.05$ ) at 2 h. Asterisk indicates that the mean rank values for treatments  $\geq 100$  µM EIP were significantly different than the mean rank values for the untreated control and 50 µM EIP ( $p < 0.05$ ). (B) Same as panel A, except for 4 h incubation time rather than 2 h. The Kruskal-Wallis test indicated a significant effect of treatment on swimming motility ( $\chi^2(5) = 40.399$ ,  $p < 0.05$ ). Asterisk indicates that the mean rank values for treatments  $\geq 100$  µM EIP were significantly different than the mean rank values for the untreated control and 50 µM EIP ( $p < 0.05$ ).

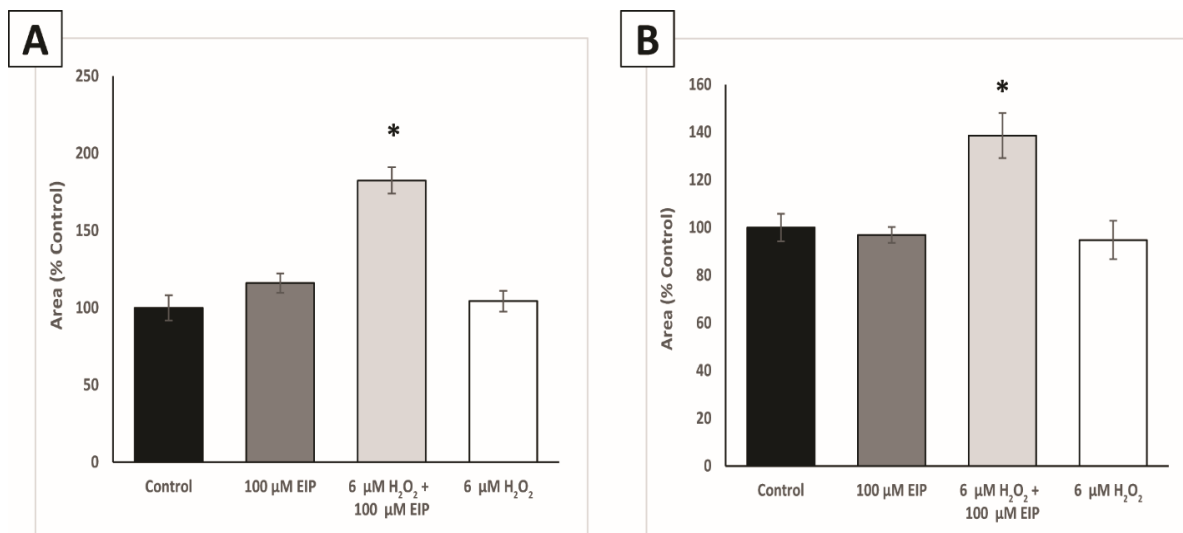


**Figure 3.6: Effects of EIP + H<sub>2</sub>O<sub>2</sub> on motility at 2 and 4 h.** (A) Effects of 6 μM H<sub>2</sub>O<sub>2</sub> + 100 μM EIP on *P. aeruginosa* swimming motility at 2 h at 37°C. Swimming motility for each treatment was quantified by measuring the diameter (mm) of each motility zone and calculating the area (mm<sup>2</sup>) of each zone after incubation. Treatments are as follows: untreated control (PBM-no glucose) (black bar), 100 μM EIP (dark gray bar), 6 μM H<sub>2</sub>O<sub>2</sub> + 100 μM EIP (light gray bar), and 6 μM H<sub>2</sub>O<sub>2</sub> (white bar). Values are means ± standard errors of the means for two replicates for each experimental condition. Treatments were normalized to untreated controls after taking the mean of the values for each of the control replicates. An independent-samples Kruskal-Wallis test indicated a significant effect of treatment on swimming motility ( $\chi^2(3) = 30.251$ ,  $p < 0.05$ ) at 2 h. Asterisk indicates that the mean rank value for the 6 μM H<sub>2</sub>O<sub>2</sub> + 100 μM EIP treatment was significantly different than the mean rank values for each compound alone and the untreated control ( $p < 0.05$ ). (B) Same as panel A, except for 4 h incubation time rather than 2 h. The Kruskal-Wallis test indicated a significant effect of treatment on swimming motility ( $\chi^2(3) = 14.530$ ,  $p < 0.05$ ) at 4 h. Asterisk indicates that the mean rank value for the 6 μM H<sub>2</sub>O + 100 μM EIP treatment was significantly different than the mean rank values for each compound alone and the untreated control ( $p < 0.05$ ).

### 3.4 Discussion

Our results show that EIP + H<sub>2</sub>O<sub>2</sub> acts in combination against *P. aeruginosa* biofilms at micromolar concentrations in two ways: prevention of biofilm formation and disruption of established biofilms. Preventing biofilm formation is an important anti-biofilm strategy, and it encompasses the use of compounds that modulate gene expression linked to virulence factors, cell-to-surface adhesion, and interference with exopolysaccharide production (71). However, in many cases, the specific mechanisms of agents that prevent biofilm formation have yet to be elucidated. The extent of biofilm inhibition caused by EIP + H<sub>2</sub>O<sub>2</sub> is similar to the biofilm inhibiting effect caused by the *Bacillus subtilis* S8-18-derived  $\alpha$ -amylase, a type of hydrolase that prevented biofilm formation in *P. aeruginosa* and other pathogens (72). As is the case with  $\alpha$ -amylases, EIP + H<sub>2</sub>O<sub>2</sub> could play a direct role in inhibiting biofilm formation by interference with bacterial adhesion, which is a critical step in initial biofilm formation and has been shown to occur within the first several hours in *P. aeruginosa* (73). There is an ecological interpretation for the biofilm prevention activity of EIP + H<sub>2</sub>O<sub>2</sub>: Escapin, the L-amino acid oxidase from which EIP is derived, is a paralog of aplysianin A, an L-amino acid oxidase used by the sea hare *A. californica* to prevent microbial biofouling of its egg capsules (28, 58, 74).

A notable finding of this work is the ability of H<sub>2</sub>O<sub>2</sub> to inhibit *P. aeruginosa* biofilm formation at micromolar concentrations. This is of particular interest due to the fact that millimolar concentrations are commonly used to trigger sublethal effects of oxidative stress in *P. aeruginosa* (75). *P. aeruginosa* is adapted to detect and overcome oxidative stress, particularly at these low millimolar concentrations (76, 77). Low millimolar concentrations of H<sub>2</sub>O<sub>2</sub> have been shown to actually enhance biofilm formation, most likely through a quorum sensing mechanism (78). Transcriptomic analyses have shown that exposure to H<sub>2</sub>O<sub>2</sub> results in an increase in mRNA levels

of genes necessary to deal with oxidative stress as well as virulence factors (75). These adaptive capabilities are not unique to *P. aeruginosa*. *Salmonella enterica* Typhimurium becomes resistant to H<sub>2</sub>O<sub>2</sub> treatments as high as 10 mM after exposure to sub-lethal concentrations of H<sub>2</sub>O<sub>2</sub> (60 μM) (79). Similar observations have also been reported in *Escherichia coli* (80). However, here we have identified concentrations of H<sub>2</sub>O<sub>2</sub> that when paired with EIP, inhibit biofilm formation at levels far below those commonly tested against *P. aeruginosa*.

Oxidizing agents such as H<sub>2</sub>O<sub>2</sub> have well-documented antimicrobial effects through DNA damage and oxygen radical toxicity (81, 82). The antimicrobial effects are often more pronounced in planktonic cells as they are genotypically and phenotypically different from their biofilm counterparts and are generally more susceptible to treatments (77, 83). In fact, this same pattern of susceptibility was observed in our antimicrobial treatment in that EIP + H<sub>2</sub>O<sub>2</sub> was more effective against planktonic cultures of *P. aeruginosa* (1, 84). In addition to inhibiting biofilm formation, the combination of EIP and H<sub>2</sub>O<sub>2</sub> is effective against established *P. aeruginosa* biofilms at micromolar concentrations, which is at or below concentrations often used in published treatment assessments. For example, Stewart *et al.* (77) showed that a steady treatment of 50 mM H<sub>2</sub>O<sub>2</sub> for 1 h had little effect on wild-type *P. aeruginosa* biofilms, a result linked to the combined effects of reduced penetration of the compound through the biofilm matrix and the protective role of catalase production in the biofilm. Similarly, Bjarnsholt *et al.* (85) treated established *P. aeruginosa* biofilms with 100 mM H<sub>2</sub>O<sub>2</sub> and demonstrated a decrease in susceptibility, most likely due to a quorum sensing mechanism. Although microbial biofilms are generally less susceptible to the effects of H<sub>2</sub>O<sub>2</sub>, specifically at concentrations in the low millimolar range, our results suggest a treatment strategy in which H<sub>2</sub>O<sub>2</sub> is effective at micromolar concentrations.

Disrupting established biofilms is a critical anti-biofilm strategy in applied contexts. Several factors promote detachment of *P. aeruginosa*, including enzymatic disruption of the surrounding extracellular polymeric substance (EPS) matrix, oxygen radical-dependent killing of bacteria (86), prophage-mediated bacterial death that enhances dispersal of cells from the biofilm (62), or the release of amyloid fibers linking cells in the biofilm together, a process regulated by D-amino acids (87). Area layer analysis indicated that introduction of EIP, either alone or in combination with H<sub>2</sub>O<sub>2</sub>, significantly affected biofilm structure down to the substratum. The fact that treatment with H<sub>2</sub>O<sub>2</sub> alone appeared to have no significant structural effect on the biofilm was not completely unexpected. In fact, H<sub>2</sub>O<sub>2</sub>-mediated cell lysis has been shown to contribute to extracellular DNA (eDNA) release in *P. aeruginosa* biofilms (88). This eDNA release, coupled with poor penetration of the H<sub>2</sub>O<sub>2</sub> through the biofilm matrix or its inactivation by catalases, could account for the largely unchanged biofilm structure, particularly at the substratum. The introduction of EIP, on the other hand, either alone or in combination with H<sub>2</sub>O<sub>2</sub>, significantly affects biofilm structure, specifically down to the substratum. EIP may not be susceptible to the same inactivation mechanisms seen with H<sub>2</sub>O<sub>2</sub>, which would allow it to penetrate and disrupt the biofilm matrix more effectively. Since previous work with EIP in planktonic cultures suggested DNA condensation as a mechanism underlying its bactericidal properties (28), we initially hypothesized that EIP may be affecting the structural stability of the biofilm matrix by targeting the eDNA. This is of particular importance because eDNA is an important structural component to *P. aeruginosa* biofilms and has been viewed as a viable target for biofilm disruption using enzymes such as DNase (89). However, the possibility of EIP initiating biofilm dispersal through a motility-dependent mechanism was also considered. Bacterial motility such as swimming, swarming (flagella-mediated) and twitching (type IV pili-mediated) are essential in *P. aeruginosa*

biofilm formation and maturation (90). In fact, the enhancement of *P. aeruginosa* motilities, such as swimming, and its subsequent role in biofilm dispersal by compounds such as nitric oxide (91) and ginseng extracts (69) are well documented. Interestingly, we determined that exposure to 1 mM EIP significantly enhances swimming motility in *P. aeruginosa* when compared to untreated controls. Follow-up experiments showed that concentrations as low as 100  $\mu$ M EIP resulted in enhanced swimming motility relative to untreated controls, while pairing of 6  $\mu$ M H<sub>2</sub>O<sub>2</sub> + 100  $\mu$ M EIP enhanced swimming motility to a greater degree than either compound alone. This effect was observed over a period of 4 h and provides further support to the effectiveness of these compounds. Altogether, the coupling of EIP with hydroxyl radicals generated by H<sub>2</sub>O<sub>2</sub>, which have also been shown to trigger DNA damage (81, 92), results in a significant dispersal effect to established *P. aeruginosa* biofilms.

There is additional significance in that the presence of endogenous H<sub>2</sub>O<sub>2</sub> in the biofilm environment has been documented. Liu *et al.* (93) measured H<sub>2</sub>O<sub>2</sub> concentrations in the range of 0.7–1.6 mM in *Streptococcus gordonii* biofilms and suggested that H<sub>2</sub>O<sub>2</sub> concentrations can vary by species composition. Likewise, many oral streptococci produce H<sub>2</sub>O<sub>2</sub> as a means of competitive advantage (94). The production of oxygen radicals, including H<sub>2</sub>O<sub>2</sub> by polymorphonuclear leukocytes (PMNs) as means of eradicating microbial infections, is yet another potential source of endogenous H<sub>2</sub>O<sub>2</sub> that could be encountered within a biofilm environment (85). Thus, introduction of EIP alone could potentially enhance the inherent disruptive effects of H<sub>2</sub>O<sub>2</sub> in these environments.

EIP + H<sub>2</sub>O<sub>2</sub> is a potentially valuable therapeutic for anti-virulence strategies, because it negatively impacts biofilm development and promotes dispersal at sub-lethal concentrations. Anti-virulence strategies are currently being pursued to overcome widespread microbial multi-

drug resistance (14). In general, these strategies aim to control microbial pathogenesis by targeting virulence mechanisms (e.g. cell adhesion, quorum sensing, biofilm formation, toxin production) while minimizing the selective pressure on the microorganisms that often leads to resistance (14, 95). Further investigation into the potential application of these compounds in combination with existing treatment strategies is both warranted and the focus of future work.

## 4 CONCLUSIONS

Over the past twenty years, microbial biofilms have been investigated for their significant impact in both clinical and industrial settings (2). The biofilm lifestyle allows microorganisms to colonize and establish complex communities in diverse environments. It is important, therefore, to understand the factors that promote biofilm formation and maturation. During the course of our investigations, we relied on methods for constructing polymicrobial biofilms with defined compositions in order to test various hypotheses regarding factors that influence biofilm establishment under antibiotic challenge. Surface colonization is an important step in the biofilm formation process. The amount of cells that colonize a given surface can ultimately affect the development of the biofilm as it matures, particularly under antibiotic pressure. Nutrient availability also plays an important role in the biofilm lifestyle. The presence or absence of nutrients can serve as an environmental cue, triggering phenotypic changes in cells that make them more or less resistant to antimicrobial treatments. Future directions taking advantage of our described methods would be ideal for studying interactions between biofilms comprised of multiple pathogens. For example, the sputum of cystic fibrosis patients has been characterized to contain pathogens such as *P. aeruginosa* and *Staphylococcus aureus* (96). Indwelling devices, such as catheters, have also been shown to be colonized by various pathogens. Thus, modeling biofilm interactions is of extreme value, taking into consideration the mounting negative impact that biofilms and antibiotic resistance have on global health.

Strategies to combat rising levels of antibiotic resistance are driven by the increases in multi-drug resistance in pathogenic bacteria. Another major part of our investigation was to determine the efficacy of the novel antimicrobial treatment combination, EIP + H<sub>2</sub>O<sub>2</sub>, towards bacterial biofilms. The combination of these compounds was previously determined to be

effective against planktonic cultures of bacteria. Using *P. aeruginosa* as a model organism, we found that combination treatments of EIP + H<sub>2</sub>O<sub>2</sub> were effective at inhibiting early biofilm formation as well as dispersal of pre-formed biofilms. A key distinction of our findings was that treatment concentrations of our compounds were effective at the micromolar range, far below the millimolar ranges previously observed on planktonic cultures. For both biofilm inhibition and biofilm dispersal, combining EIP + H<sub>2</sub>O<sub>2</sub> was more effective than each compound alone, suggesting a synergistic interaction between the compounds. Inhibition was observed during early biofilm formation (< 4 h) at nearly 70% of untreated controls. Biofilm dispersal of 24 h biofilms was observed at nearly 40% of untreated controls after only a 30 min treatment. The role of EIP as a potential novel treatment strategy is particularly attractive due to its synergistic activity with H<sub>2</sub>O<sub>2</sub>, especially at low concentrations. Hydrogen peroxide is readily encountered in microbial environments, particularly at wound sites, and therefore it may be possible to deliver EIP to wound sites and allow it to work with endogenous concentrations of H<sub>2</sub>O<sub>2</sub>.

Based on calculated ratios of membrane damage (live/dead staining), we were able to determine that dispersal was not due to a bactericidal effect of the compounds. In the absence of a bactericidal effect to account for dispersal, we hypothesized that a motility mechanism may be responsible for the dispersal activity. This enhancement in motility was observed while performing motility assays, where combined treatments of EIP + H<sub>2</sub>O<sub>2</sub>, both at micromolar concentrations, resulted in increased swimming motility. Future work should take these observations into account when establishing a clearer mechanism of action of our treatments, particularly against other well-known pathogens. Additionally, future work should focus on the use of these compounds as possible adjuvants in combination with current antibiotic treatments. Potentiating antibiotics, potentially reducing the effective doses of current treatments, would add

yet another tool in the toolbox for combatting the impact of antibiotic resistance. Overall, the application of EIP + H<sub>2</sub>O<sub>2</sub> as an antibiofilm agent is quite promising.

## REFERENCES

1. **Ko K-C, Wang B, Tai PC, Derby CD.** 2008. Identification of Potent Bactericidal Compounds Produced by Escapin, an l-Amino Acid Oxidase in the Ink of the Sea Hare *Aplysia californica*. *Antimicrobial Agents and Chemotherapy* **52**:4455-4462.
2. **Costerton JW, Lewandowski Z, Caldwell DE, Korber DR, Lappin-Scott HM.** 1995. Microbial Biofilms. *Annual Review of Microbiology* **49**:711-745.
3. **Zambrano MM, Kolter R.** 2005. Mycobacterial Biofilms: A Greasy Way to Hold It Together. *Cell* **123**:762-764.
4. **Flemming H-C, Neu TR, Wozniak DJ.** 2007. The EPS Matrix: The “House of Biofilm Cells”. *Journal of Bacteriology* **189**:7945-7947.
5. **Flemming H-C, Wingender J.** 2010. The Biofilm Matrix. *Nature Reviews in Microbiology* **8**:623-633.
6. **Hall-Stoodley L, Costerton JW, Stoodley P.** 2004. Bacterial Biofilms: From the Natural Environment to Infectious Diseases. *Nature Reviews in Microbiology* **2**:95-108.
7. **Videla HA.** 2002. Prevention and Control of Biocorrosion. *International Biodeterioration & Biodegradation* **49**:259-270.
8. **Kumar CG, Anand SK.** 1998. Significance of Microbial Biofilms in Food Industry: A Review. *International Journal of Food Microbiology* **42**:9-27.
9. **Bryers JD.** 2008. Medical Biofilms. *Biotechnology and Bioengineering* **100**:1-18.
10. **Tomasz A.** 1997. Antibiotic Resistance in *Streptococcus pneumoniae*. *Clinical Infectious Diseases* **24**:S85-S88.
11. **Barbosa TM, Levy SB.** 2000. The Impact of Antibiotic Use on Resistance Development and Persistence. *Drug Resistance Updates* **3**:303-311.
12. **Neu HC.** 1992. The Crisis in Antibiotic Resistance. *Science* **257**:1064-1073.
13. **Samore MH, Magill MK, Alder SC, Severina E, Morrison-de Boer L, Lyon JL, Carroll K, Leary J, Stone MB, Bradford D, Reading J, Tomasz A, Sande MA.** 2001. High Rates of Multiple Antibiotic Resistance in *Streptococcus pneumoniae* From Healthy Children Living in Isolated Rural Communities: Association With Cephalosporin Use and Intrafamilial Transmission. *Pediatrics* **108**:856-865.
14. **Cegelski L, Marshall GR, Eldridge GR, Hultgren SJ.** 2008. The Biology and Future Prospects of Antivirulence Therapies. *Nature Reviews in Microbiology* **6**:17-27.
15. **Panmanee W, Taylor D, Shea CJA, Tang H, Nelson S, Seibel W, Papoian R, Kramer R, Hassett DJ, Lamkin TJ.** 2013. High-Throughput Screening for Small-Molecule Inhibitors of *Staphylococcus epidermidis* RP62a Biofilms. *Journal of Biomolecular Screening* **18**:820-829.
16. **Chaignon P, Sadovskaya I, Ragunah C, Ramasubbu N, Kaplan JB, Jabbouri S.** 2007. Susceptibility of *Staphylococcal* Biofilms to Enzymatic Treatments Depends on their Chemical Composition. *Applied Microbiology and Biotechnology* **75**:125-132.
17. **Stobie N, Duffy B, McCormack DE, Colreavy J, Hidalgo M, McHale P, Hinder SJ.** 2008. Prevention of *Staphylococcus epidermidis* Biofilm Formation Using a Low-Temperature Processed Silver-Doped Phenyltriethoxysilane Sol–Gel Coating. *Biomaterials* **29**:963-969.
18. **Harris LG, Tosatti S, Wieland M, Textor M, Richards RG.** 2004. *Staphylococcus aureus* Adhesion to Titanium Oxide Surfaces Coated with Non-Functionalized and

- Peptide-Functionalized Poly(L-Lysine)-Grafted-Poly(Ethylene Glycol) Copolymers. *Biomaterials* **25**:4135-4148.
19. **Mühlen S, Dersch P.** 2016. Anti-virulence Strategies to Target Bacterial Infections, p 1-37, *Current Topics in Microbiology and Immunology* doi:10.1007/82\_2015\_490. Springer Berlin Heidelberg, Berlin, Heidelberg.
  20. **Niu C, Gilbert ES.** 2004. Colorimetric Method for Identifying Plant Essential Oil Components That Affect Biofilm Formation and Structure. *Applied and Environmental Microbiology* **70**:6951-6956.
  21. **Rossi M, Heuertz R.** 2015. Cinnamaldehyde Inhibits Biofilm Formation of MRSA. *The FASEB Journal* **29**:1 Supplement 575.579.
  22. **Brackman G, Defoirdt T, Miyamoto C, Bossier P, Van Calenbergh S, Nelis H, Coenye T.** 2008. Cinnamaldehyde and Cinnamaldehyde Derivatives Reduce Virulence in *Vibrio* spp. by Decreasing the DNA-binding Activity of the Quorum Sensing Response Regulator LuxR. *BMC Microbiology* **8**:149.
  23. **Okubo BM, Silva ON, Migliolo L, Gomes DG, Porto WF, Batista CL, Ramos CS, Holanda HHS, Dias SC, Franco OL, Moreno SE.** 2012. Evaluation of An Antimicrobial L-Amino Acid Oxidase and Peptide Derivatives from *Bothropoides matogrosensis* Pitviper Venom. *PLoS ONE* **7**:e33639.
  24. **Kasai K, Ishikawa T, Komata T, Fukuchi K, Chiba M, Nozaka H, Nakamura T, Sato T, Miura T.** 2010. Novel L-Amino Acid Oxidase with Antibacterial Activity Against Methicillin-Resistant *Staphylococcus aureus* Isolated from Epidermal Mucus of the Flounder *Platichthys stellatus*. *FEBS Journal* **277**:453-465.
  25. **Yang H, Johnson PM, Ko K-C, Kamio M, Germann MW, Derby CD, Tai PC.** 2005. Cloning, Characterization and Expression of Escapin, a Broadly Antimicrobial FAD-Containing L-Amino Acid Oxidase from Ink of the Sea Hare *Aplysia californica*. *Journal of Experimental Biology* **208**:3609-3622.
  26. **Peters BM, Jabra-Rizk MA, O'May GA, Costerton JW, Shirtliff ME.** 2012. Polymicrobial Interactions: Impact on Pathogenesis and Human Disease. *Clinical Microbiology Reviews* **25**:193-213.
  27. **Hoffman LR, D'Argenio DA, MacCoss MJ, Zhang Z, Jones RA, Miller SI.** 2005. Aminoglycoside Antibiotics Induce Bacterial Biofilm Formation. *Nature* **436**:1171-1175.
  28. **Ko K-C, Tai PC, Derby CD.** 2012. Mechanisms of Action of Escapin, a Bactericidal Agent in the Ink Secretion of the Sea Hare *Aplysia californica*: Rapid and Long-Lasting DNA Condensation and Involvement of the OxyR-Regulated Oxidative Stress Pathway. *Antimicrobial Agents and Chemotherapy* **56**:1725-1734.
  29. **Costerton JW, Stewart PS, Greenberg EP.** 1999. Bacterial Biofilms: A Common Cause of Persistent Infections. *Science* **284**:1318-1322.
  30. **Flemming H-C.** 2002. Biofouling in Water Systems – Cases, Causes and Countermeasures. *Applied Microbiology and Biotechnology* **59**:629-640.
  31. **Wagner VE, Iglewski BH.** 2008. *P. aeruginosa* Biofilms in CF Infection. *Clinical Reviews in Allergy & Immunology* **35**:124-134.
  32. **Trautner BW, Darouiche RO.** 2004. Catheter-Associated Infections: Pathogenesis Affects Prevention. *Archives of Internal Medicine* **164**:842-850.
  33. **Højby N, Bjarnsholt T, Givskov M, Molin S, Ciofu O.** 2010. Antibiotic Resistance of Bacterial Biofilms. *International Journal of Antimicrobial Agents* **35**:322-332.

34. **Ito A, Taniuchi A, May T, Kawata K, Okabe S.** 2009. Increased Antibiotic Resistance of *Escherichia coli* in Mature Biofilms. *Applied and Environmental Microbiology* **75**:4093-4100.
35. **Guo K, Freguia S, Dennis PG, Chen X, Donose BC, Keller J, Gooding JJ, Rabaey K.** 2013. Effects of Surface Charge and Hydrophobicity on Anodic Biofilm Formation, Community Composition, and Current Generation in Bioelectrochemical Systems. *Environmental Science & Technology* **47**:7563-7570.
36. **Renner LD, Weibel DB.** 2011. Physicochemical Regulation of Biofilm Formation. *MRS bulletin / Materials Research Society* **36**:347-355.
37. **Lasaro MA, Salinger N, Zhang J, Wang Y, Zhong Z, Goulian M, Zhu J.** 2009. F1C Fimbriae Play an Important Role in Biofilm Formation and Intestinal Colonization by the *Escherichia coli* Commensal Strain Nissle 1917. *Applied and Environmental Microbiology* **75**:246-251.
38. **Saginur R, StDenis M, Ferris W, Aaron SD, Chan F, Lee C, Ramotar K.** 2006. Multiple Combination Bactericidal Testing of *Staphylococcal* Biofilms from Implant-Associated Infections. *Antimicrobial Agents and Chemotherapy* **50**:55-61.
39. **Stubblefield BA, Howery KE, Islam BN, Santiago AJ, Cardenas WE, Gilbert ES.** 2010. Constructing Multispecies Biofilms with Defined Compositions by Sequential Deposition of Bacteria. *Applied Microbiology and Biotechnology* **86**:1941-1946.
40. **O'Connell HA, Kottkamp GS, Eppelbaum JL, Stubblefield BA, Gilbert SE, Gilbert ES.** 2006. Influences of Biofilm Structure and Antibiotic Resistance Mechanisms on Indirect Pathogenicity in a Model Polymicrobial Biofilm. *Applied and Environmental Microbiology* **72**:5013-5019.
41. **O'Connell HA, Kottkamp GS, Eppelbaum JL, Stubblefield BA, Gilbert SE, Gilbert ES.** 2006. Influences of biofilm structure and antibiotic resistance mechanisms on indirect pathogenicity in a model polymicrobial biofilm. *Appl Environ Microbiol* **72**:5013-5019.
42. **Gilbert ES, Keasling JD.** 2004. Bench Scale Flow Cell for Nondestructive Imaging of Biofilms, p 109-118. In Walker JM, Spencer JFT, Ragout de Spencer AL (ed), *Environmental Microbiology: Methods and Protocols* doi:10.1385/1-59259-765-3:109. Humana Press, Totowa, NJ.
43. **Heydorn A, Nielsen AT, Hentzer M, Sternberg C, Givskov M, Ersbøll BK, Molin S.** 2000. Quantification of Biofilm Structures by the Novel Computer Program Comstat. *Microbiology* **146**:2395-2407.
44. **He H, Cooper JN, Mishra A, Raskin DM.** 2012. Stringent Response Regulation of Biofilm Formation in *Vibrio cholerae*. *Journal of Bacteriology* **194**:2962-2972.
45. **Boehm A, Steiner S, Zaehring F, Casanova A, Hamburger F, Ritz D, Keck W, Ackermann M, Schirmer T, Jenal U.** 2009. Second Messenger Signalling Governs *Escherichia coli* Biofilm Induction Upon Ribosomal Stress. *Molecular Microbiology* **72**:1500-1516.
46. **Lewis K.** 2007. Persister Cells, Dormancy and Infectious Disease. *Nature Reviews in Microbiology* **5**:48-56.
47. **Barraud N, Buson A, Jarolimek W, Rice SA.** 2013. Mannitol Enhances Antibiotic Sensitivity of Persister Bacteria in *Pseudomonas aeruginosa* Biofilms. *PLoS ONE* **8**:e84220.

48. **Halan B, Buehler K, Schmid A.** 2012. Biofilms as Living Catalysts in Continuous Chemical Syntheses. *Trends in Biotechnology* **30**:453-465.
49. **Joseph B, Otta SK, Karunasagar I, Karunasagar I.** 2001. Biofilm Formation by *Salmonella* spp. on Food Contact Surfaces and their Sensitivity to Sanitizers. *International Journal of Food Microbiology* **64**:367-372.
50. **Hatt JK, Rather PN.** 2008. Role of Bacterial Biofilms in Urinary Tract Infections, p 163-192. In Romeo T (ed), *Bacterial Biofilms* doi:10.1007/978-3-540-75418-3\_8. Springer Berlin Heidelberg, Berlin, Heidelberg.
51. **Donlan RM.** 2008. Biofilms on Central Venous Catheters: Is Eradication Possible?, p 133-161. In Romeo T (ed), *Bacterial Biofilms* doi:10.1007/978-3-540-75418-3\_7. Springer Berlin Heidelberg, Berlin, Heidelberg.
52. **Kilb B, Lange B, Schaule G, Flemming H-C, Wingender J.** 2003. Contamination of Drinking Water by Coliforms from Biofilms Grown On Rubber-Coated Valves. *International Journal of Hygiene and Environmental Health* **206**:563-573.
53. **Simões M, Simões LC, Vieira MJ.** 2010. A Review of Current and Emergent Biofilm Control Strategies. *LWT - Food Science and Technology* **43**:573-583.
54. **Derby CD, Aggio JF.** 2011. The Neuroecology of Chemical Defenses. *Integrative and Comparative Biology* **51**:771-780.
55. **Walters ET, Erickson MT.** 1986. Directional Control and the Functional Organization of Defensive Responses in *Aplysia*. *Journal of Comparative Physiology A* **159**:339-351.
56. **Nolen TG, Johnson PM.** 2001. Defensive Inking in *Aplysia* spp: Multiple Episodes of Ink Secretion and the Adaptive Use of a Limited Chemical Resource. *Journal of Experimental Biology* **204**:1257-1268.
57. **Kicklighter CE, Shabani S, Johnson PM, Derby CD.** 2005. Sea Hares Use Novel Antipredatory Chemical Defenses. *Current Biology* **15**:549-554.
58. **Derby CD.** 2007. Escape by Inking and Secreting: Marine Molluscs Avoid Predators Through a Rich Array of Chemicals and Mechanisms. *The Biological Bulletin* **213**:274-289.
59. **Johnson PM, Kicklighter CE, Schmidt M, Kamio M, Yang H, Elkin D, Michel WC, Tai PC, Derby CD.** 2006. Packaging of Chemicals in the Defensive Secretory Glands of the Sea Hare *Aplysia californica*. *Journal of Experimental Biology* **209**:78-88.
60. **Kamio M, Ko K-C, Zheng S, Wang B, Collins SL, Gadda G, Tai PC, Derby CD.** 2009. The Chemistry of Escapin: Identification and Quantification of the Components in the Complex Mixture Generated by an L-Amino Acid Oxidase in the Defensive Secretion of the Sea Snail *Aplysia californica*. *Chemistry – A European Journal* **15**:1597-1603.
61. **Toté K, Berghe DV, Deschacht M, de Wit K, Maes L, Cos P.** 2009. Inhibitory Efficacy of Various Antibiotics on Matrix and Viable Mass of *Staphylococcus aureus* and *Pseudomonas aeruginosa* Biofilms. *International Journal of Antimicrobial Agents* **33**:525-531.
62. **Whiteley M, Bangera MG, Bumgarner RE, Parsek MR, Teitzel GM, Lory S, Greenberg EP.** 2001. Gene Expression in *Pseudomonas aeruginosa* Biofilms. *Nature* **413**:860-864.
63. **Musken M, Di Fiore S, Romling U, Haussler S.** 2010. A 96-Well-Plate-Based Optical Method for the Quantitative and Qualitative Evaluation of *Pseudomonas aeruginosa* Biofilm Formation and its Application to Susceptibility Testing. *Nature Protocols* **5**:1460-1469.

64. **Atlas RM.** 2004. *Handbook of Microbiological Media (3rd ed.)*. CRC Press, Boca Raton, FL.
65. **Lu SP, Lewin AH.** 1998. Enamine/imine Tautomerism in  $\alpha,\beta$ -unsaturated- $\alpha$ -amino acids. *Tetrahedron* **54**:15097-15104.
66. **Merritt JH, Kadouri DE, O'Toole GA.** 2005. Growing and Analyzing Static Biofilms, *Current Protocols in Microbiology* doi:10.1002/9780471729259.mc01b01s00. John Wiley & Sons, Inc.
67. **O'Toole GA, Pratt LA, Watnick PI, Newman DK, Weaver VB, Kolter R.** 1999. [6] Genetic Approaches to Study of Biofilms, p 91-109, *Methods in Enzymology*, vol Volume 310. Academic Press.
68. **Pittman KJ, Robbins CM, Osborn jL, Stubblefield BA, Gilbert ES.** 2010. Agarose Stabilization of Fragile Biofilms for Quantitative Structure Analysis. *Journal of Microbiological Methods* **81**:101-107.
69. **Wu H, Lee B, Yang L, Wang H, Givskov M, Molin S, Høiby N, Song Z.** 2011. Effects of Ginseng on *Pseudomonas aeruginosa* Motility and Biofilm Formation. *FEMS Immunology & Medical Microbiology* **62**:49-56.
70. **Rashid MH, Kornberg A.** 2000. Inorganic Polyphosphate is Needed for Swimming, Swarming, and Twitching Motilities of *Pseudomonas aeruginosa*. *Proceedings of the National Academy of Sciences USA* **97**:4885-4890.
71. **Chen M, Yu Q, Sun H.** 2013. Novel Strategies for the Prevention and Treatment of Biofilm Related Infections. *International Journal of Molecular Sciences* **14**:18488–18501.
72. **Kalpana BJ, Aarthy S, Pandian SK.** 2012. Antibiofilm Activity of  $\alpha$ -Amylase from *Bacillus subtilis* S8-18 Against Biofilm Forming Human Bacterial Pathogens. *Applied Biochemistry and Biotechnology* **167**:1778-1794.
73. **Rasamiravaka T, Labtani Q, Duez P, El Jaziri M.** 2015. The Formation of Biofilms by *Pseudomonas aeruginosa*: A Review of the Natural and Synthetic Compounds Interfering with Control Mechanisms. *BioMed Research International* **2015**:1-17.
74. **Cummins SF, Nichols AE, Amare A, Hummon AB, Sweedler JV, Nagle GT.** 2004. Characterization of *Aplysia* Enticin and Temptin, Two Novel Water-borne Protein Pheromones That Act in Concert with Attractin to Stimulate Mate Attraction. *Journal of Biological Chemistry* **279**:25614-25622.
75. **Palma M, DeLuca D, Worgall S, Quadri LEN.** 2004. Transcriptome Analysis of the Response of *Pseudomonas aeruginosa* to Hydrogen Peroxide. *Journal of Bacteriology* **186**:248-252.
76. **Lee J-S, Heo Y-J, Lee JK, Cho Y-H.** 2005. KatA, the Major Catalase, Is Critical for Osmoprotection and Virulence in *Pseudomonas aeruginosa* PA14. *Infection and Immunity* **73**:4399-4403.
77. **Stewart PS, Roe F, Rayner J, Elkins JG, Lewandowski Z, Ochsner UA, Hassett DJ.** 2000. Effect of Catalase on Hydrogen Peroxide Penetration into *Pseudomonas aeruginosa* Biofilms. *Applied and Environmental Microbiology* **66**:836-838.
78. **Plyuta VA, Andreenko JV, Kuznetsov AE, Khmel' IA.** 2013. Formation of *Pseudomonas aeruginosa* PAO1 Biofilms in the Presence of Hydrogen Peroxide. The Effect of the *aiiA* Gene. *Molecular Genetics, Microbiology and Virology* **28**:141-146.

79. **Christman MF, Morgan RW, Jacobson FS, Ames BN.** 1985. Positive Control of a Regulon for Defenses Against Oxidative Stress and Some Heat-Shock Proteins in *Salmonella typhimurium*. *Cell* **41**:753-762.
80. **Demple B, Halbrook J.** 1983. Inducible Repair of Oxidative DNA Damage in *Escherichia coli*. *Nature* **304**:466-468.
81. **Imlay J, Linn S.** 1988. DNA Damage and Oxygen Radical Toxicity. *Science* **240**:1302-1309.
82. **Kasai K, Ishikawa T, Nakamura T, Miura T.** 2015. Antibacterial Properties of L-Amino Acid Oxidase: Mechanisms of Action and Perspectives for Therapeutic Applications. *Applied Microbiology and Biotechnology* **99**:7847-7857.
83. **Perumal PK, Wand ME, Sutton JM, Bock LJ.** 2014. Evaluation of the Effectiveness of Hydrogen-Peroxide-Based Disinfectants on Biofilms Formed by Gram-Negative Pathogens. *Journal of Hospital Infection* **87**:227-233.
84. **Ko K-C.** 2011. Bactericidal Mechanisms of Escapin, A Protein in the Ink of a Sea Hare. Dissertation. Georgia State University, Atlanta, GA.
85. **Bjarnsholt T, Jensen PØ, Burmølle M, Hentzer M, Haagensen JAJ, Hougen HP, Calum H, Madsen KG, Moser C, Molin S, Høiby N, Givskov M.** 2005. *Pseudomonas aeruginosa* Tolerance to Tobramycin, Hydrogen Peroxide and Polymorphonuclear Leukocytes is Quorum-Sensing Dependent. *Microbiology* **151**:373-383.
86. **Meyle E, Stroh P, Günther F, Hoppy-Tichy T, Wagner C, Hänsch GM.** 2010. Destruction of Bacterial Biofilms by Polymorphonuclear Neutrophils: Relative Contribution of Phagocytosis, DNA Release, and Degranulation. *The International Journal of Artificial Organs* **33**:608-620.
87. **Kolodkin-Gal I, Romero D, Cao S, Clardy J, Kolter R, Losick R.** 2010. D-Amino Acids Trigger Biofilm Disassembly. *Science* **328**:627-629.
88. **Das T, Manefield M.** 2012. Pyocyanin Promotes Extracellular DNA Release in *Pseudomonas aeruginosa*. *PLoS ONE* **7**:e46718.
89. **Whitchurch CB, Tolker-Nielsen T, Ragas PC, Mattick JS.** 2002. Extracellular DNA Required for Bacterial Biofilm Formation. *Science* **295**:1487-1487.
90. **O'Toole GA, Kolter R.** 1998. Flagellar and Twitching Motility are Necessary for *Pseudomonas aeruginosa* Biofilm Development. *Molecular Microbiology* **30**:295-304.
91. **Barraud N, Hassett DJ, Hwang S-H, Rice SA, Kjelleberg S, Webb JS.** 2006. Involvement of Nitric Oxide in Biofilm Dispersal of *Pseudomonas aeruginosa*. *Journal of Bacteriology* **188**:7344-7353.
92. **Imlay J, Chin S, Linn S.** 1988. Toxic DNA Damage by Hydrogen Peroxide Through the Fenton Reaction *in vivo* and *in vitro*. *Science* **240**:640-642.
93. **Liu X, Ramsey MM, Chen X, Koley D, Whiteley M, Bard AJ.** 2011. Real-Time Mapping of a Hydrogen Peroxide Concentration Profile Across a Polymicrobial Bacterial Biofilm Using Scanning Electrochemical Microscopy. *Proceedings of the National Academy of Sciences USA* **108**:2668-2673.
94. **Zhu L, Kreth J.** 2012. The Role of Hydrogen Peroxide in Environmental Adaptation of Oral Microbial Communities. *Oxidative Medicine and Cellular Longevity* **2012**:1-10.
95. **Tay S, Yew W.** 2013. Development of Quorum-Based Anti-Virulence Therapeutics Targeting Gram-Negative Bacterial Pathogens. *International Journal of Molecular Sciences* **14**:16570-16599.

96. **Costerton JW.** 2001. Cystic Fibrosis Pathogenesis and the Role of Biofilms in Persistent Infection. *Trends in Microbiology* **9**:50-52.